Global Change Biology

WILEY

Global Change Biology

RESEARCH ARTICLE OPEN ACCESS

Limitation of Maize Potential Yield by Phosphorus at the Global Scale

B. Ringeval[1] | J. Demay[1] | J. Helfenstein[2] | M. Kvakić[3] | A. Mollier[1] | M. Seghouani[4] | T. Nesme[1] | J. S. Gerber[5] | N. D. Mueller[6] | S. Pellerin[1]

[1]ISPA, Bordeaux Sciences Agro, INRAE, Villenave d'Ornon, France | [2]Soil Geography and Landscape Group, Wageningen University & Research, Wageningen, the Netherlands | [3]Croatian Meteorological and Hydrological Service, Zagreb, Croatia | [4]LAE, Universite de Lorraine, INRAE, Colmar, France | [5]Institute on the Environment, University of Minnesota, St Paul, Minnesota, USA | [6]Department of Ecosystem Science and Sustainability, Department of Soil and Crop Sciences, Colorado State University, Fort Collins, Colorado, USA

Correspondence: B. Ringeval (bruno.ringeval@inrae.fr)

Received: 19 May 2025 | **Revised:** 18 August 2025 | **Accepted:** 18 August 2025

Keywords: crop model | nutrient cycling | optimal function | phosphorus limitation | yield gap | *Zea mays*

ABSTRACT

Phosphorus (P) is known as a major limiting factor of crop yields at the global scale. Previous estimates of the global P limitation are either based on statistical approaches or on complex global gridded crop models. Both failed to distinguish between P and the other limiting factors. Global gridded crop models, despite their complexities, omitted key mechanisms such as soil P dynamics or plant adjustments to P limitation (e.g., change in root:shoot ratio or in shoot P concentration). Thus, current approaches fail to quantify the contribution of P limitation to the global yield gap. Here, we developed a simple but mechanistic model (called GPCROP) that simulates the interactions between plant growth and soil P at a daily time step, all other factors being assumed non-limiting. The model explicitly represents key mechanisms such as the replenishment of the soil P solution by more stable soil P pools, the diffusion of P in soil, and plant adjustments to P limitation. We found that soil available P greatly limits the global maize potential production, even when that limitation was strongly alleviated by plant adjustment mechanisms. With and without these adjustments, maize global production would decrease by 78.9% (std = 17.3) and 92.7% (std = 7.4), respectively, compared to its potential production. We also found that the beginning of the growing season is a key period for P limitation as roots, not yet developed, cannot sustain the plant P demand. This suggests that earlier studies based on a comparison between annual averages of soil supply versus plant demand are not appropriate for assessing P limitation. Considerable uncertainties remain in our approach, and we especially stress the need to use global datasets of soil iron and aluminum (hydr)oxides, currently in development, to constrain the spatial variation of some key parameters driving the P concentration of the soil solution.

1 | Introduction

Phosphorus (P) is one of the key limitations to crop yields (Mueller et al. 2012). This is because in most soils, the amount of total P is low or because P is present in forms that are not available for plants (Walker and Syers 1976). In agroecosystems, the export of P due to harvesting tends to increase the soil P limitation. On the other side, soil P inputs as chemical fertilizers or manure can reach consequential values, sometimes above plant P uptake leading to the accumulation of P in soils (Margenot et al. 2024). P contained in chemical fertilizers is derived from apatite mining, and access to these resources is becoming increasingly uncertain due to limited rock phosphate supplies and potential geopolitical rivalries (Obersteiner et al. 2013; Elser and Bennett 2011). P resource management is far from optimal at the global scale. For example, in the 2000s, while global soil P inputs through chemical and organic fertilizers were larger than the P contained in global harvests, around 30% of the cropland

area had a negative local soil P budget (MacDonald et al. 2011). However, the annual soil P budget is only a partial indicator of the P limitation as, contrary to nitrogen, P is a non-mobile element in soil, leading to the necessity to take into account past soil P budgets (so-called "residual" P when these budgets are positive; Sattari et al. 2012; Margenot et al. 2024), the soil biogeochemical background, and soil P dynamics (Ringeval et al. 2017).

Orthophosphate ions (the only form of P taken up by plants) are easily adsorbed on soil particles, which makes their concentration in soil solution very low (Helfenstein, Jegminnat, et al. 2018). In such cases, diffusion is the major mechanism for transport in soil, and the replenishment of the soil solution from P sorbed on soil particles is a key process in plant P nutrition. The way to represent such replenishment at large spatial scales remains challenging because of its reliance on conventional soil tests and chemical extractions, which are poorly mechanistic and do not represent the same P forms across pedo-climatic contexts (Helfenstein, Tamburini, et al. 2018; Wang et al. 2022).

Despite the importance of soil P for crop yield, the relationship between soil P and yield is far from understood at the global scale, given difficulties in global soil P mapping (Helfenstein et al. 2024), the above-mentioned intrinsic complexities of P cycle modeling, and spatially variable interactions between P and other determinants of yield gaps (nitrogen, water, pest and diseases). In the literature, different approaches aim to represent the limitation of the yield by nutrients at the global scale. They can be based on statistics (Mueller et al. 2012; McDowell et al. 2024), or on dataset manipulation, e.g., by computing historical soil nutrient budgets (Bouwman et al. 2017). Such soil P budgets have been combined with a very simple soil P dynamic model (Sattari et al. 2012; Zhang et al. 2017) within the so-called IMAGE-DPPS model in order to investigate the P limitation of yield under current conditions (Langhans et al. 2021) and future scenarios (Mogollón et al. 2018, 2021; Magnone et al. 2019, 2022). None of the above-mentioned studies explicitly represent plant growth: For example, McDowell et al. (2024) used, for each crop, a soil labile P value beyond which yield is assumed not to be limited. Besides, two kinds of mechanistic modeling approaches representing plant growth in agroecosystems at the global scale have been developed: (i) terrestrial biosphere models, historically focused on natural ecosystems, but more recently incorporated managed agroecosystems and P cycle representation (e.g., Sun et al. 2021) and (ii) crop models initially used at the field scale and more recently upscaled to the global scale. These two approaches are usually merged in what is called "Global Gridded Crop Models" (GGCMs) (Elliott et al. 2015). These GGCMs are important tools, in particular to quantify the effect of climate change or scenarios of resource management (water, nitrogen, land-use) on global crop production (Rosenzweig et al. 2014), to understand mechanisms at play under such changes/scenarios (Martre et al. 2024) and to investigate how different sustainability objectives can be reconciled (Folberth et al. 2020; Gerten et al. 2020). However, GGCMs have some caveats. First, few GGCMs explicitly represent P limitation on vegetation growth (Müller et al. 2019). Second, the complexities of GGCMs make specifically investigating P limitation difficult. Third, GGCMs are prone to huge heterogeneity in the simulation of key variables such as potential yield (Ringeval et al. 2021). Last, some mechanisms can be poorly represented: e.g., plant adjustment mechanisms to nutrient limitation (change in root:shoot ratio, variable organ nutrient concentration) are only considered in few terrestrial biosphere models (Zaehle and Dalmonech 2011). Only a few studies involving GGCMs have been done up to now to investigate the P limitation (Folberth et al. 2012, 2013; van der Velde et al. 2014; Kvakić et al. 2018) with most of them based on the EPIC models family in which soil P dynamics are roughly represented.

To better understand the P limitation of crop yield at the global scale, we developed here a simple and mechanistic approach (called GPCROP), independent to any GGCM, to simulate the interaction between plant growth and soil P at daily time-step for 1 year. The model assumes no other limitation (such as water or nitrogen), and this assumption is made for each spatial unit of the model. Following this assumption, our approach allows quantifying the P limitation of potential yield by the current soil P status. We deliberately choose to exclude other limiting factors to remove any difficulties related to interactions between P and other factors and to focus on P as a first step. What we call here "potential yield" corresponds to the "attainable yield" defined by Gerber et al. (2024) to estimate the highest yield attained somewhere in the world in each set of biophysical conditions, which likely remains 15%–25% below the true agronomic potential. GPCROP was calibrated in order that the yield simulated without P limitation matches the spatial distribution of empirically-derived potential yield (Gerber et al. 2024). Simulations are performed for maize at half-degree latitude × longitude spatial resolution. Maize is chosen because of its key contribution to the global cropland area and calories intake (Shiferaw et al. 2011). GPCROP makes possible the consideration of key mechanisms involved in plant limitation by P. In particular, the soil P dynamics model allows to represent the replenishment of the soil P solution, the parametrization of the P supply by roots allows to represent the diffusion of P in soil and the allocation model, based on an optimization procedure, allows to represent plant adjustments to P limitation such as change in root:shoot ratio and change in leaf P concentration. In this paper, we first describe the model. Then, we analyze the model behavior on a given site where a long-term P fertilization experiment was conducted. Finally, we investigate our model results at the global scale.

2 | Methods

2.1 | Overview

In the present study, we coupled, after slight modification, a simple mechanistic model (called SIM) that simulates the potential (i.e., without any limitation) biomass and yield of maize at a daily time step (Ringeval et al. 2021) to (i) a model describing the allocation of carbon (C) and P among plant organs based on an optimization procedure (inspired by Kvakić et al. 2020), (ii) the computation of P supply by roots and P demand to sustain plant growth (following Kvakić et al. 2018) and (iii) a soil P dynamics model (called GPASOIL, Ringeval et al. 2024) (Figure 1).

Each day, in case P supply is smaller than P demand, the plant is P limited and the allocation scheme allows us to represent

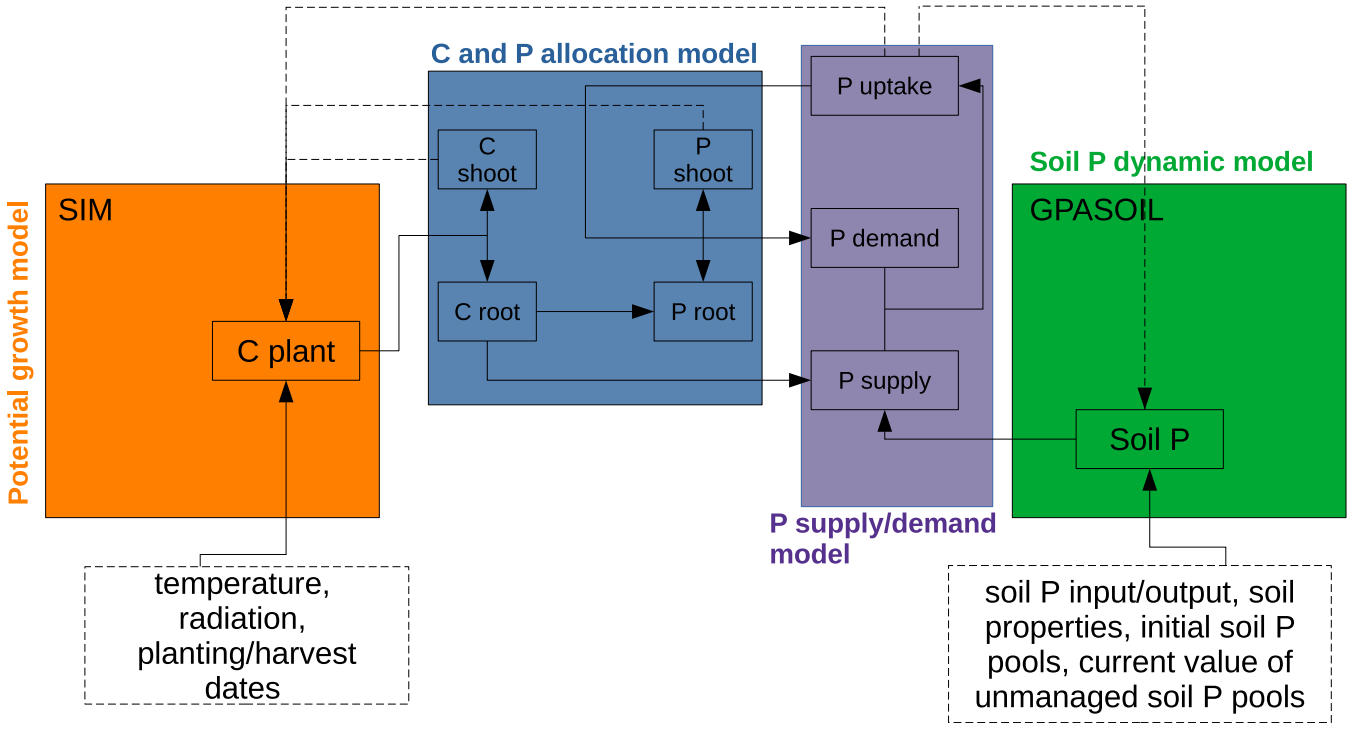

FIGURE 1 | General view of the model coupling. SIM (orange box), GPASOIL (green box), a model describing the allocation of C (or biomass) and P among plant organs (blue box) and parametrizations for P demand and P supply (purple box) are coupled to build GPCROP. Model input are given in dash boxes. Main feedbacks are given with dashed arrows: Plant P uptake determines how much biomass can be fixed, both biomass allocation towards shoot and P shoot concentration has an effect on photosynthesis, and P uptake can modify soil P. Grain is not distinguished from shoot in the figure.

some plant adjustments to alleviate the P limitation: increase in root:shoot ratio (to increase the P supply) and decrease of P leaf concentration (to decrease the P demand). Here we assumed that trends observed at the seasonal time scale for root:-shoot ratio and leaf P concentration (Amos and Walters 2006; Plénet et al. 2000) can be reproduced by changes in allocation occurring at the daily time step. In case P supply is larger than P demand, growth is not P limited and the optimized allocation leads to potential crop growth. The actual daily plant P uptake (derived from P supply and P demand) decreases the inorganic labile P pool, which is then replenished by the other soil P pools, as computed by the soil P dynamics model. The P supply is a function of the P concentration of the soil solution (computed with GPASOIL) and the root biomass. Its computation allows consideration of the diffusive transport of P up to the soil-root interface. The P demand corresponds to the P needed by the plant for the daily increment of its different organs. It is a function of daily change in biomass of each organ and organ P concentration. The P concentration of root and grain are constant while the concentration of shoot (excluding grain) is optimized. The allocation scheme of biomass (or C) and P reproduces some trade-offs at the plant level: (i) the more the biomass is allocated to leaves, the more the plant can photosynthesize but the less P can be taken up by roots; (ii) a higher P concentration in leaves increases photosynthesis but increases the P demand to sustain the plant growth. Each day, the optimization procedure makes all processes considered (photosynthesis, P uptake, allocation, plant growth) consistent with each other.

In Ringeval et al. (2021), SIM was used as an emulator of Global Gridded Crop Models (GGCMs) to understand their differences in the simulation of potential yield. Here, the potential yield was calibrated against empirically-derived potential yield given by Gerber et al. (2024). Given the large discrepancy in GGCMs simulation of potential yield (see figure 1 of Ringeval et al. 2021), we chose here to rely on empirically-derived yield, despite its own sources of uncertainty. No constraints about the cultivar distribution were used as input of SIM. Instead, we let the calibration determines the spatial distribution of the SIM parameters, most of which are related to cultivar properties. GPASOIL has been evaluated by comparing the spatial distribution of simulated soil P against regional databases in Ringeval et al. (2024). The comparison concerned soil P pools extracted with different chemical extractions (Hedley for the simulation vs. e.g., Olsen for the observations) and that is why it focused on the *relative* spatial distribution (Ringeval et al. 2024). This evaluation showed room for improvement, though with some difficulties to track the reasons for the mismatch between simulations and observations (possible reasons include the lack of oxalate-extractable iron and aluminium to estimate the parameters involved in soil P dynamics, difficulties in computing accurate soil P budgets, uncertainties related to the use of the different dataset for the evaluation). Initial soil P pools at the beginning of the year were provided by Ringeval et al. (2024) and GPASOIL is here used to compute the daily exchange between inorganic labile P and other soil P pools after the plant P uptake allowing the pools to vary during the growing season.

The allocation scheme is inspired from Kvakić et al. (2020) and was evaluated against observations in both hydroponic experiments and in a long-term field trial in the original study. As this scheme has been modified in the current study, in particular to allow its coupling with SIM and P uptake computation, we evaluated again how GPCROP reproduces the effect of a gradient of P limitation on yield against observations at a long-term field trial.

In our modeling approach, each organ is characterized by its biomass ($biom_{organ}$) (expressed in gDM m^{-2}) and P content ($biomP_{organ}$) (expressed in gP m^{-2}). Plants are restricted to three organs only: shoot excluding grain (called hereafter "swog" for Shoot WithOut Grain), grain and root. Total shoot biomass and total shoot P content are defined as:

$$biom_{shoot}(d) = biom_{swog}(d) + biom_{grain}(d) \quad (1)$$

$$biomP_{shoot}(d) = biomP_{swog}(d) + biomP_{grain}(d) \quad (2)$$

Stem and leaf are not explicitly distinguished in GPCROP. For each organ, the ratio of P content and biomass defines the P concentration ($conc_{organ}$, expressed here in gP gDM^{-1}):

$$conc_{organ}(d) = \frac{biomP_{organ}(d)}{biom_{organ}(d)} \quad (3)$$

An additional pool of plant P reserve, $biomP_{res}$, is also considered and acts as a buffering pool receiving P at leaf senescence before its potential remobilization the day after.

Variables vary in time (i.e., are a function of day d) while parameters are constant in time. Both variables and parameters (after calibration, see later) vary in space as a function of grid-cells but this dependency is not specified in the equations for purpose of simplicity.

2.2 | Model Description

2.2.1 | Computation of Climate Forcing

GPCROP focused on the growing season, defined by the time-period between the planting day (t_p, in day) and the day of crop maturity/harvest (t_m, in day). For a given day d of the growing season, the thermal time (TT, in °C) is computed from the daily mean temperature (tas, in °C) by using three references temperatures (T_{min}, T_{opt}, T_{max}, in °C):

$$TT(d) = \begin{cases} 0 & \text{if } tas(d) \le T_{min} \text{ or } tas(d) \ge T_{max} \\ tas(d) - T_{min} & \text{if } T_{min} < tas(d) \le T_{opt} \\ \frac{T_{min} - T_{opt}}{T_{max} - T_{opt}}\left(tas(d) - T_{max}\right) & \text{if } T_{opt} < tas(d) < T_{max} \end{cases} \quad (4)$$

Through these equations, we assumed a linear increase of TT from T_{min} to T_{opt} followed by a linear decrease up to T_{max}.

We defined GDD_{remain} (in °C d) as the sum of growing degree days since the last leaf emergence:

$$GDD_{remain}(d) = GDD_{remain}(d-1) + TT(d) \quad (5)$$

The use of a sum of growing degree days since the last leaf emergence (insead of a sum since the beginning of the growing season, as in the original SIM; Ringeval et al. 2021) is only a strategy for facilitating the coupling with daily P limitation. The reset of the sum of growing degree days after leaf emergence is performed each day, after optimization (see Section 2.2.4).

The incoming photosynthetic active radiation (PAR_{inc}, in MJ m^{-2} day^{-1}) is derived from the short-wave downwelling radiation (rsds, in MJ m^{-2} day^{-1}) and its active fraction ($frac_{PAR}$, no unit).

$$PAR_{inc}(d) = frac_{PAR} \times rsds(d) \quad (6)$$

2.2.2 | Optimization Procedure

The objective function, for any day d, is:

$$\text{Maximize} \quad \left(biom_{shoot}(d)\right) \quad (7)$$

Optimizations are described through a set of constraints that are verified simultaneously. Equations given below are used as constraints of our optimization procedure. All variables of day d are output from the optimization except: $GDD_{remain}(d)$, $frac_{grain}(d)$ (fraction of total NPP dedicated to the grain filling) and $C_P(d)$ (P concentration of soil solution) that are input of the optimization procedure (Section 2.2.4). All variables of the day (d−1) are inputs to the optimization.

The first constraint allows us to define the daily increment of biomass between two consecutive days for any organ within {shoot, swog, grain, root}:

$$\Delta biom_{organ}(d) = biom_{organ}(d) - biom_{organ}(d-1) \quad (8)$$

Within the optimization procedure, $\Delta biom_{organ}$ is still positive or nul. The senescence of leaves can decrease biomass (and thus lead to negative $\Delta biom_{organ}$) but in GCPROP, this process is treated outside of the optimization at the end of each day (Section 2.2.4). The number of leaves (n_{leaf}, no unit) and leaf area index (LAI, no unit) are provided by the following set of constraints:

$$n_{leaf}(d) \le n_{leaf}(d-1) + \frac{GDD_{remain}(d)}{GDD_{1leaf}} \quad (9)$$

$$n_{leaf}(d) \ge n_{leaf}(d-1) \quad (10)$$

$$n_{leaf,wosene}(d) - n_{leaf,wosene}(d-1) = n_{leaf}(d) - n_{leaf}(d-1) \quad (11)$$

$$n_{leaf,wosene}(d) \le \max_{nleaf} \quad (12)$$

$$LAI(d) = LAI(d-1) + a_{LAI}\left(e^{b_{LAI}.n_{leaf,wosene}(d)} - e^{b_{LAI}.n_{leaf,wosene}(d-1)}\right) \quad (13)$$

$$LAI(d) \le LAI(d-1) + SLA.\,\Delta biom_{shoot}(d) \quad (14)$$

where GDD_{1leaf} is a parameter representing the thermal requirement for the emergence of any leaf (in °C d), max_{nleaf} is the maximum number of leaves that can emerge per plant in the course of a growing season (no unit), SLA is a specific leaf area (in $m^2\,gDM^{-1}$), a_{LAI} and b_{LAI} (no unit) are parameters that link exponentially the LAI and the number of leaves. $n_{leaf,wosene}$ ("wosene" for "without senescence") is similar to n_{leaf} except that leaf senescence has no effect on $n_{leaf,wosene}$. Equation (11) allows $n_{leaf,wosene}$ and n_{leaf} to evolve similarly in time through the optimization. The effect of the senescence on n_{leaf} is introduced outside of the optimization procedure (Section 2.2.4). Equation (12) concerns the variable $n_{leaf,wosene}$ (instead of n_{leaf}); thus, it prevents the emergence of a total number of leaves larger than max_{nleaf} through the whole growing season whatever senescence occurs or not. Equation (9) represents the limitation by thermal requirement while (Equation 14) represents the carbohydrates limitation as in Mollier et al. (2008). Equation (14) was missing in SIM and was here introduced to allow a negative feedback of allocation towards the root (instead of the shoot) when the root:shoot ratio is allowed to vary. We assumed SLA as constant in time (see general discussion).

The net primary productivity (NPP_{tot}, in $gDM\,m^{-2}\,day^{-1}$) is computed with the following constraints:

$$PUE(d) = \frac{conc_{swog}(d) - conc_{swog,def}}{\left(conc_{swog,def} - conc_{swog,min}\right).\left(1 - \alpha_{PUE}\right)} + 1 \quad (15)$$

$$NPP_{tot}(d) \le PUE(d).\,RUE_{tot}.\,PAR_{inc}(d).\left(1 - e^{-k_{ext}.LAI(d)}\right) \quad (16)$$

$$NPP_{tot}(d) = \Delta biom_{root}(d) + \Delta biom_{shoot}(d) \quad (17)$$

with PUE (P use efficiency, no unit) is a variable representing the effect of the P concentration of shoot excluding grain ($conc_{swog}$) on the NPP, RUE_{tot} is a radiation use efficiency (in $gDM\,MJ^{-1}$ of absorbed PAR), and k_{ext} is the light extinction coefficient (no unit). The subscript "tot" means that we focus here on the total NPP (and not on the NPP alllocated to the aboveground plant only). $conc_{swog}(d)$ varies between a minimum concentration ($conc_{swog,min}$) and a default concentration ($conc_{swog,def}$). The sensitivity of NPP to P leaf concentration is subject to debate (e.g., Plénet et al. 2000; Ellsworth et al. 2022) and we choose here to introduce a linear sensitivity of PUE to $conc_{swog}$ but with three different values of α_{PUE} in our uncertainty analysis (see Section 2.5.4). If $conc_{swog}$ is equal to the default value ($conc_{swog,def}$), PUE is equal to 1 whatever α_{PUE}, and α_{PUE} determines the rate of the decrease in PUE when $conc_{swog}$ is below the default value (Figure S1). The inequality (16) means that NPP which is not fixed because of P limitation is lost. Equation (17) means that all NPP is either attributed to increment of biomass of root or shoot. Consistently with an optimization procedure, the above constraints governing n_{leaf} and NPP are considered simultaneously. How these equations can be translated into successive equations (without optimization) is described in Appendix S1.

The biomass of grain is computed thanks to:

$$\Delta biom_{grain}(d) = frac_{grain}(d).\,NPP_{tot}(d) \quad (18)$$

where $frac_{grain}$ is the fraction of NPP allocated to the grain (no unit, see its computation in Section 2.2.4).

P in biomass are given by:

$$biomP_{organ}(d) = biomP_{organ}(d-1) + \Delta biom_{organ}(d).\,conc_{\Delta organ}(d) \quad (19)$$

where $conc_{\Delta organ}(d)$ are the P concentration of the increment of biomass of day d. As the P concentration of root and grain are constant in time, we have for any day d:

$$conc_{\Delta root}(d) = conc_{root}(d) \quad (20)$$

$$conc_{\Delta grain}(d) = conc_{grain}(d) \quad (21)$$

while the P concentration of the total shoot excluding grain ($conc_{swog}(d)$) or of the daily increment ($conc_{\Delta swog}(d)$) are allowed to vary during the optimization within given ranges:

$$conc_{\Delta swog,min} \le conc_{\Delta swog}(d) \le conc_{\Delta swog,def} \quad (22)$$

$$conc_{swog,min} \le conc_{swog}(d) \le conc_{swog,def} \quad (23)$$

We arbitrarily set:

$$conc_{\Delta swog,min} = \frac{conc_{swog,min}}{2} \quad (24)$$

$$conc_{\Delta swog,def} = conc_{swog,def} \times 2 \quad (25)$$

to allow a larger range (i.e., more flexibility) for $conc_{\Delta swog}$ than for $conc_{swog}$.

Similarly, the root:shoot ratio is allowed to vary within a given range:

$$RSR_{def} \le \frac{biom_{root}(d)}{biom_{shoot,wosene}(d)} \le RSR_{max} \quad (26)$$

where $biom_{shoot,wosene}$ is similar to $biom_{shoot}$ except that leaf senescence has no effect on $biom_{shoot,wosene}$:

$$biom_{shoot,wosene}(d) - biom_{shoot,wosene}(d-1) = biom_{shoot}(d) - biom_{shoot}(d-1) \quad (27)$$

P demand and P supply (in $gP\,m^{-2}\,day^{-1}$) are defined through the following constraints:

$$P_{demand}(d) = \sum_{organ \in \{swog,grain,root\}} \left(\Delta biom_{organ}(d).\,conc_{\Delta organ}(d)\right) \quad (28)$$

$$P_{supply}(d) = f_{Taylor}\left(biom_{root}(d), C_P(d)\right) \quad (29)$$

P supply depends on root biomass ($biom_{root}$) and P concentration of soil solution C_P according to the non-linear equation given in the next section. As the optimization used is a linear optimization, only linear relationships between variables optimized are allowed. Thus, a Taylor series at order 1 around $biom_{root}(d-1)$ and $C_P(d-1)$ of the (Equation 33) was used instead of (Equation 33) itself. This Taylor series is called f_{Taylor} in the above constraint. Similarly, constraints 13 (about LAI

computation as function of number of leaves), 16 (about NPP), 19 for shoot excluding grain (the relationship between concentration of total organ and daily biomass increment) and 28 (about P demand) were linearized.

The mass conservation of P is guaranteed through:

$$P_{uptake}(d) = \Delta biomP_{root}(d) + \Delta biomP_{shoot}(d) + \Delta biomP_{res}(d) \quad (30)$$

where P_{uptake} is the P uptake (in gP m^{-2} day^{-1}).

The following set of constraints make biomass growth and P interact:

$$P_{demand}(d) \leq P_{supply}(d) - \Delta biomP_{res}(d) \quad (31)$$

$$P_{uptake}(d) \leq P_{demand}(d) \quad (32)$$

with the daily increment of reserve ($\Delta biomP_{res}(d)$) being negative or null. The P uptake is the minimum value between the P demand and the P supply (after substracting the P reserve from the P supply). The above constraints, if removed, make biomass grow without any P limitation (Section 2.3).

The optimization is used for the whole growing season but not before $n_{leaf,wosene}$ is greater or equal to a given threshold, called $n_{leaf,thresh}$. For $n_{leaf,wosene} \leq n_{leaf,thresh}$, plant growth is not limited by P.

To solve the linear programming problem, we used the python package "pulp" and BCB MILP solver. Taylor series is computed thanks to the package "sympy".

2.2.3 | P Supply Computation

For each day d, the P supply (in gP m^{-2} day^{-1}) depends on the root biomass and the P concentration of soil solution. Following the zero-sink uptake assumption (Mollier et al. 2008; Willigen and Noordwijk 1994), the P supply is given by the equation used in Kvakić et al. (2018):

$$P_{supply}(d) = 1e^3 . \pi . \Delta z . L_{rv}(d) . D . \frac{\rho(d)^2 - 1}{G_\rho(d)} . C_P(d) \quad (33)$$

with $1e^3$ is a scaling factor (in L m^{-3}), Δz is the thickness of the top soil horizon considered (in m, $\Delta z = 0.3$ m), L_{rv} is the root length density (i.e., the length of root per volume of soil, in (m of root) (m of soil)$^{-3}$), D is the P diffusivity in soil (in (m of soil)^2 day^{-1}), G_ρ is a dimensionless geometric function of a ratio of soil cylinder to root radius (ρ, dimensionless), and C_P is the mean concentration of orthophosphate ions of the soil solution in Δz (in gP L^{-1}), provided by the soil P dynamics model.

The root length density is computed as follows:

$$L_{rv}(d) = \frac{biom_{root}(d) . SRL}{\Delta z} \quad (34)$$

where $biom_{root}$ is the root biomass, SRL is the specific root length (in m gDM^{-1}).

The P diffusivity in soil is computed using the methods of Barraclough and Tinker (1981) following Mollier et al. (2008). The formula used here was determined by the fact that the soil water content is above a given threshold because we assumed here the field capacity to approach potential growth conditions. Following Mollier et al. (2008), G_ρ has a simplified formula in case of P for which diffusion is the main process of transport in soil. Thus, G_ρ depends on ρ only, which is the normalized ratio of soil cylinder to root radius (no unit), expressed as:

$$\rho(d) = \frac{1}{R_0 . \sqrt{\pi . L_{rv}(d)}} \quad (35)$$

The parameter R_0 is the root radius (in m) and is part of the uncertainty analysis (Section 2.5.4). SRL is set to 100 m gDM^{-1}. More details about P supply computation are given in Appendix S2.

2.2.4 | Mechanisms Related to Plant Growth Simulated Outside of the Optimization Procedure

Each day, after the optimization is solved, some other mechanisms are simulated within GPCROP. These include an update of GDD_{remain}, the computation of the fraction of NPP allocated to the grain (f_{grain}) as well as the leave senescence and associated P remobilization.

2.2.4.1 | Update of GDD_{remain}. GDD_{remain} is modified as follows:

$$GDD_{remain}(d) = GDD_{remain}(d) - GDD_{1leaf} . \left(n_{leaf}(d) - n_{leaf}(d-1)\right) \quad (36)$$

$$GDD_{remain}(d) = \min\left(GDD_{remain}(d), GDD_{1leaf}\right) \text{ if } n_{leaf} < \max_{nleaf} \quad (37)$$

The first equation allows us to remove the sum of growing degree days used for the emergence of leaves during day d. The second equation prevents accumulation of GDD above GDD_{1leaf} when leaf cannot emerge on day d despite thermal requirement satisfied due to either carbohydrate limitation (Equation 14) or P limitation. Such accumulation of GDD would allow the emergence of many leaves at the same day once the P limitation is alleviated.

2.2.4.2 | Computation of the Fraction of NPP Allocated to the Grain. The grain-filling starts the day after the emergence of the last leaf (i.e., the leaf number $\max_{nleaf}$):

$$frac_{grain}(d) = \begin{cases} 0 & \text{if } n_{leaf,wosene}(d-1) < \max_{nleaf} \\ f_{grain} & \text{if } n_{leaf,wosene}(d-1) = \max_{nleaf} \end{cases} \quad (38)$$

Once grain filling starts, a constant fraction of NPP is allocated to grain (see Equation 18).

2.2.4.3 | Senescence and P Remobilization. In GPCROP, a leaf dies as soon as the GDD cumulated since its emergence reaches the value given by the parameter GDD_{life} (in °C d). Between day (d−1) and day d, we assumed that GDD does not accumulate if n_{leaf} does not increase between those 2 days

and this is done to postpone senescence in case of severe P limitation that halt growth. We called $n_{leaf,dead}(d)$ the number of leaves that dead during the day d due to senescence, and $LAI_{dead}(d)$ the amount of LAI corresponding to $n_{leaf,dead}(d)$. The effect of senescence is computed as follows:

$$n_{leaf}(d) = n_{leaf}(d) - n_{leaf,dead}(d) \quad (39)$$

$$LAI(d) = LAI(d) - LAI_{dead}(d) \quad (40)$$

$$biom_{swog}(d) = biom_{swog}(d) - \frac{LAI_{dead}(d)}{SLA} \quad (41)$$

Through (Equation 41), we assumed that leaf biomass decreases proportionally to SLA. An alternative would be to decrease the biomass proportionally to the ratio $n_{leaf,dead}(d)/n_{leaf}(d)$. In the model, senescence can start before the grain filling but we prevent senescence to decrease n_{leaf} below 1 to prevent instability in the optimization procedure the day after.

This decrease in shoot excluding grain biomass is translated into a transfer of P to P reserves:

$$biomP_{res}(d) = biomP_{res}(d) + \frac{LAI_{dead}(d) \times conc_{swog}(d)}{SLA} \quad (42)$$

and $biomP_{res}(d)$ can be used in the optimization procedure of the next day, instead of P uptake. It corresponds to P remobilization that we assume is only driven by senescence in our approach.

In addition to a straightforward decrease in biomass, it is worth noting that the senescence has also an indirect effect on the biomass through the effect of the decrease in LAI on the NPP of the following days.

2.2.5 | Soil P Dynamics

Soil P dynamics were simulated with GPSAOIL, described in Ringeval et al. (2024) and summarized in Appendix S3. Seven soil P pools were considered following the merging of Hedley fractions (table 9 of Ringeval et al. 2024): P_{i-sol} (inorganic P in soil solution), P_{i-lab} (labile inorganic P), P_{i-sec} (moderately labile inorganic P), P_{i-prim} (primary inorganic P), P_{o-lab} (labile organic P), P_{i-sta} (stable organic P), P_{x-occ} (occluded P), with the first letter in subscript refers to inorganic (i), organic (o) or inorganic+organic (x). Soil P pools are expressed here in gP m^{-2}.

Parameters involved in inorganic soil P pool exchanges (called k-parameters hereafter) were similar to the ones used in Ringeval et al. (2024). They rely on the pedo-climatic relationships provided by Wang et al. (2022) after modifications described in Ringeval et al. (2024): namely, all k-parameters are constant in time, and oxalate-extractable iron and alumnium are excluded from parametrization due to lack of global data on these soil properties. As a result, the model operates with simplified equations for k parameters and an equilibrium P concentration of the soil solution ($C_{P,\infty}$, called $P_{c,\infty}$ in Ringeval et al. 2024), which is constant in space. Fluxes from organic to inorganic pools follows first order kinetics with residence times of 15 and 2 year. for P_{o-sta} and P_{o-lab}, respectively (corresponding to the so-called version 1.1 of GPASOIL in Ringeval et al. 2024).

GPASOIL is here used to compute the daily exchange between inorganic labile P and other soil P pools following plant P uptake. Each day, the soil P pool P_{i-lab} is first modified according to the P uptake:

$$P_{i-lab}(d) = P_{i-lab}(d) - P_{uptake}(d).\Delta t \quad (43)$$

with Δt equals to 1 day. Then the soil P dynamics is computed (thanks to GPASOIL) within the same day to allow P_{i-sol}, P_{i-lab} and P_{i-sec} (among others) to exchange after P uptake. The P uptake is removed from P_{i-lab} and not from P_{i-sol} as it is usually larger than P_{i-sol} at daily time-step.

The P concentration of the soil solution is used in GPASOIL equations to derive the exchange between soil solution and other soil P pools (Appendix S3) and is also needed to compute P supply (Equation 33). It is derived from P_{i-sol} and the soil water content. Here, as we focus on potential crop growth without considering limitations other than P, we prescribed the soil water content (θ, in $m^3\ m^{-3}$) to its field capacity (θ_{fc}, in $m^3\ m^{-3}$):

$$C_P(d) = 1e^{-3}.\frac{P_{i-sol}(d)}{\theta(d).\Delta z} \quad (44)$$

$$\theta(d) = \theta_{fc} \quad (45)$$

with $1e^{-3}$ is a scaling factor (in $m^3\ L^{-1}$).

2.3 | GPCROP Configurations

Three alternative GPCROP configurations were defined to investigate the effect of P limitation on potential crop yield. In the first one, called $GPCROP_{no-intera}$, there is no interaction between plant growth and P limitation: in such case, plant can grow without being limited by P. Yield at harvest simulated with this configuration corresponds to the potential yield. This configuration is defined by removing the constraints 31–32 in GPCROP. In that case, P uptake is equal to the P demand and is not limited by soil P, and optimization procedure leads to both root:shoot ratio and $conc_{swog,min}$ equal to their respective default value (RSR_{def} and $conc_{swog,def}$, respectively).

In the second configuration, called $GPCROP_{non-optim}$, the optimization procedure is used to deal with the interactions between plant growth and P limitation but the plant can optimize neither its root:shoot ratio nor the P concentration of shoot without grain. The constraints 31–32 are considered but RSR_{max} and $conc_{swog,min}$ are set to RSR_{def} and $conc_{swog,def}$, respectively in Equations (23) and (26). In this configuration, both the root:shoot ratio and the P concentration of shoot without grain are constant in time. It is worth remembering that interaction between plant growth and P limitation only occur from $n_{leaf,wosene} \geq n_{leaf,thresh}$.

In the third configration, called $GPCROP_{optim}$, plant growth can be limited by P limitation as with $GPCROP_{non-optim}$ but in this configuration, the plant can optimize both its root:shoot ratio

TABLE 1 | GPASOIL and GPCROP parameters considered in the study.

Name	Meaning in the model	Unit	Comments about the value(s) chosen	Values tested at Tartas site	Values kept at Tartas site to asses the uncertainty	Values considered to assess uncertainty at the global scale
RSR_{def}	Default root: shoot ratio	—	Representative to root: shoot ratio at maturity in Amos and Walters (2006)	0.16	0.16	0.16
RSR_{max}	Maximum root: shoot ratio allowed during the optimization with $GPCROP_{optim}$	—	Maximum value found in Amos and Walters (2006) (corresponding to value at emergence)	0.68	0.68	0.68
$conc_{swog,def}$	Default P concentration of shoot excluding grain	gP gDM^{-1}	The value found at Tartas for this organ at harvest for P3 is $1.8e^{-3}$.	$2.0e^{-3}$, $3.0e^{-3}$, $4.0e^{-3}$	$2.0e^{-3}$, $3.0e^{-3}$	$2.0e^{-3}$, $3.0e^{-3}$
$conc_{swog,min}$	Minimum P concentration of shoot excluding grain allowed during the optimization with $GPCROP_{optim}$	gP gDM^{-1}	Close to the value observed at Tartas at harvest for P0 ($0.4e^{-3}$) and to the value derived from Lun et al. (2018) (given per unit of fresh matter) for maize residues at harvest time ($0.7e^{-3}$)	$0.5e^{-3}$	$0.5e^{-3}$	$0.5e^{-3}$
$conc_{grain}$	P concentration of grain	gP gDM^{-1}	Close to the value observed at Tartas at harvest for P1.5 and to the value derived from Lun et al. (2018) (given per unit of fresh matter) for maize yield at harvest time ($2.0e^{-3}$).	$2.6e^{-3}$	$2.6e^{-3}$	$2.6e^{-3}$
$conc_{root}$	P concentration of root	gP gDM^{-1}	Value of $1.1e^{-3}$ is found when average different values (silking/maturity × high/low P conditions × genotypes) provided by Sun et al. (2023)	$0.8e^{-3}$, $1.2e^{-3}$	$0.8e^{-3}$, $1.2e^{-3}$	$0.8e^{-3}$, $1.2e^{-3}$
α_{PUE}	Constant describing the linear relationship between PUE and $conc_{swog}$	No unit	Poor knowledge on the relationship between photosynthesis and leaf P concentration. Different values were tested (Figure S1b)	0.0, 0.5, 0.9	0.0, 0.5	0.0, 0.5

(Continues)

TABLE 1 | (Continued)

Name	Meaning in the model	Unit	Comments about the value(s) chosen	Values tested at Tartas site	Values kept at Tartas site to asses the uncertainty	Values considered to assess uncertainty at the global scale
t_{spinup}	Length of the spin-up for soil P dynamics before the start of the growing season	Days	Spin-up used to reach the equilibirum in soil P pools following the change from the soil water content used in Ringeval et al. (2024) and the one used in the current study (field capacity). Soil properties have been also modified for the simulations on site.	50	50	50
t_{ings}	Delay between soil P input/output (fertilizers, etc.) and the beginning of the growing season	days	Value of 20 days provided for Tartas in Plénet et al. (2000). No information could be used at the global scale.	20	20	5, 30
$n_{leaf,thresh}$	Threshold in the number of leaves from which the optimization starts. Thus, it is also the threshold from which the P limitation can occur in the model.	No unit	The stage of 3 leaves was found as transition between autotrophic and heterotrophic periods in Nadeem et al. (2014).	2, 3, 4	2, 3	2, 3
R_0	Averaged root radius	m	Close to the range of values found by Li et al. (2017) (under different sampling depths and perpendicular distance to the corn row).	$0.24e^{-3}$, $0.28e^{-3}$, $0.32e^{-3}$	$0.24e^{-3}$, $0.28e^{-3}$, $0.32e^{-3}$	$0.24e^{-3}$, $0.28e^{-3}$, $0.32e^{-3}$
$C_{P,\infty}$	P concentration of the soil solution at equilibrium	gP L^{-1}	$C_{P,\infty}$ was calibrated at Tartas site to mimic soil P concentrations observed. At the global scale, two values were used to assess the uncertainty: the same value as the one used in Tartas simulation and the default value used in Ringeval et al. (2024)	$0.35e^{-3}$	$0.35e^{-3}$	$0.10e^{-3}$, $0.35e^{-3}$

Note: Only $C_{P,\infty}$ is a parameter related to GPASOIL, with all others are related to GPCROP. From the column "values tested at Tartas site" to the column "values kept at Tartas site to asses the uncertainty", we excluded one value for α_{PUE} (0.9) and one value for $conc_{swog,default}$ ($4.0e^{-3}$ gP gDM^{-1}) as they lead to overestimate the P limitation as compared to the observations (Section 3.2). Parameters values considered to assess the uncertainty at the global scale are similar to the one used at Tartas after this exclusion, except for parameters for which a constraint could be derived from observations at Tartas but does not make sense at the global scale (t_{ings}, $C_{P,\infty}$).

and the P concentration of shoot without grain. Values of RSR_{max} and $conc_{swog,min}$ given in Table 1 are used in Equations (23) and (26), respectively.

2.4 | Calibration of Crop Growth Without P Limitation

Contrary to what was done in Ringeval et al. (2021), we aimed here to calibrate crop growth without P limitation against empirically-derived potential yield given by Gerber et al. (2024). Thus, $GPCROP_{no-intera}$ is used for the calibration and we only focus here on parameters involved in the crop growth (i.e., not on parameters involved in P supply, P demand, nor soil P dynamics). These parameters are given in Table 2 and are called SIM parameters in the following. While they have been written as constraints of an optimization procedure, the equations used to simulate biomass growth (without P limitation) given in the previous section are similar to the model SIM described in Ringeval et al. (2021), with yet some differences: first, a number of leaves limited by carbohydrates was introduced (Equation 14). Second, the parameterization in Ringeval et al. (2021) allows the start of the grain filling at different leaf numbers, as a function of the GGCM they aimed to emulate. Here, the grain filling starts after the emergence of the last leaf. Third, we introduced here a computation of

TABLE 2 | List of parameters involved in the modeling of plant growth without P limitation (i.e., SIM) and values tested in both the Sobol analysis and SIM parameters calibration.

Name	Meaning	Unit	Range of values tested	Participate to the Sobol analysis	Participate to the calibration at both site and global scales
T_{min}	Base temperature	°C	3.0–10.0	Yes	Yes
T_{max}	Threshold temperature from which TT is set to 0.	°C	38.0–45.0	Yes	No
T_{opt}	Optimum temperature, i.e., the temperature at which TT is maximum	°C	21.0–37.0	Yes	Yes
max_{nleaf}	Maximum number of leaves per plant	—	15.0–21.0	Yes	Yes
GDD_{1leaf}	Sum of growing degree day required for each leaf (so called phyllochron)	°C d	25.0–65.0	Yes	Yes
a_{LAI}	Parameter involved in the relationship between LAI and $n_{leaf,wosene}$	—	0.027–0.047	Yes	No
b_{LAI}	Parameter involved in the relationship between LAI and $n_{leaf,wosene}$	—	0.266	No	No
$frac_{PAR}$	Active fraction of short-wave down-ward radiation	—	0.48	No	No
k_{ext}	Coefficient of extinction of radiation in canopy	—	0.30–0.50	Yes	No
RUE_{tot}	Radiation use efficiency	gDM MJ^{-1} (of absorded PAR)	3.4–4.7	Yes	Yes
RSR_{def}	Default root: shoot ratio	—	0.16	No	No
f_{grain}	Fraction of daily total NPP directed towards the grain as soon as grain filling starts	—	0.40–0.80	Yes	Yes
SLA	Specific leaf area	m^2 gDM^{-1}	0.015–0.055	Yes	Yes
GDD_{life}	GDD cumulated since the emergence of a leave at which senescence occurs	°C d	700–1300	Yes	Yes

Note: For the calibration, if a parameter is calibrated, 3 values were tested and correspond to the boundaries of the range provided in the Table as well as the middle of the range. Following the Sobol analysis, few parameters were excluded from the calibration.

leaf senescence to capture the impacts of the P remobilization. Fourth, total NPP is here considered instead of aboveground NPP in Ringeval et al. (2021) as the latter study does not focus on root which was excluded of the list of variables studied in the GGCM intercomparison. Last, while the increase of thermal time from T_{min} is not limited in Ringeval et al. (2021), we introduced here T_{opt} and T_{max}.

If the constraints 31–32 are not considered, 14 parameters are involved in the computation of potential yield: T_{min}, T_{max}, T_{opt}, $frac_{PAR}$, max_{nleaf}, GDD_{1leaf}, a_{LAI}, b_{LAI}, k_{ext}, RUE_{tot}, RSR_{def}, f_{grain}, SLA, and GDD_{life}. The active fraction of short-wave downward radiation ($frac_{PAR}$) is physically well-known and was set to 0.48. RSR_{def} was not calibrated here as it is the focus of the optimization procedure with $GPCROP_{optim}$. b_{LAI} was not calibrated as the relationship between LAI and n_{leaf} was assessed through a_{LAI} (Table 2, Figure S1). Other parameters were considered uncertain and the model global sensitivities to these parameters were estimated with a global sensitivity (Sobol) analysis. The range of values allowed for each parameter is given in Table 2 and discussed in Table S1. Once the Sobol was performed, we excluded from the following calibration the parameters that have a small effect on the yield sensitivity. We call x the number of parameters that remains after the Sobol analysis and that are the focus of the calibration. The calibration relies on 3^x simulations corresponding to all combinations possible (x parameters with 3 values allowed per parameter). The 3 values tested are: minimum, middle and maximum value of the range defined for each parameter (Table 2). In all simulations, uncalibrated parameters were set to their middle value. For each simulation, each parameter was constant in space (i.e., all grid-cells share the same value). Then we combined these simulations to calibrate each grid-cell independently. For any grid-cell g, among the 3^x combinations, we keep all parameter combinations that lead to an absolute difference with a target yield at harvest lower than 50 gDM m^{-2} (or 0.5 tDM ha^{-1}) corresponding to around 7% in average, i.e., for any grid-cell g, a parameter combination is kept if it allows that:

$$\left| \mathrm{biom}_{\mathrm{grain}}^{\mathrm{target}}(g, t_m) - \mathrm{biom}_{\mathrm{grain}}(g, t_m) \right| < 50 \text{ gDM m}^{-2} \quad (46)$$

with $biomg_{grain}$ is the grain biomass computed with (Equation 18) and t_m (no unit) is the day of crop maturity/harvest.

Yield targets are different for GPCROP simulations performed at site or global scales (see next section).

2.5 | GPCROP Simulations

2.5.1 | Model Input and Overview of the Simulations

GPCROP inputs are: planting day (t_p, no unit), day of crop maturity/harvest (t_m, no unit), daily short-wave downwelling radiation (rsds, in MJ m^{-2} day^{-1}), daily mean temperature (tas, in °C), cropland soil P pools at the beginning of the year and soil P input (through mineral fertilizer, manure, atmospheric deposition and sludges) for the year considered. Soil properties and the current value of unmanaged soil P pools are also used as input of GPCROP as they are needed in the parameterizations describing the exchanges between soil P pools within GPASOIL. Potential yield at harvest ($biom_{grain}^{target}$) is used for calibration of SIM parameters. GPCROP will be used to perform both site-scale and global simulations. Input datasets and information required for each kind of simulation are described in Table 3. At site scale, $biom_{grain}^{target}$ corresponds to yield measured in the treatment without P limitation (so-called P3 in the following) for the year 1996. At the global scale, $biom_{grain}^{target}$ is provided by Gerber et al. (2024) for the year 2009, translated into gDM m^{-2} by using a dry fraction of fresh matter of 0.89. The Gerber et al. (2024) yield corresponds to «climate-specific» attainable yields, and is calculated using a quantile regression model based on weather, soil, and irrigation data trained on over 11,300 independent yield values. Because this is an empirically derived model, the yield values correspond to yields that are "attainable" using current technology, variety, management techniques and economic incentives (in contrast to agronomic yield potentials).

GPCROP simulations were performed for one growing season at daily time-step. Soil input (mineral fertilizer, manure, atmospheric deposition, sludges from waste treatment) and P losses through erosion were added to initial soil P pools at the day $d = t_p - t_{ings}$, that is, t_{ings} days before the planting day. The parameter t_{ings} is set to 20 days for site simulations following information in Plénet et al. (2000). In the global simulations, two values (5 and 30 days) were tested as source of uncertainty (Section 2.5.4). The modeling of soil P dynamics starts at the day $d = t_p - t_{spinup}$, that is, t_{spinup} days before the planting day. We set t_{spinup} equal to 50 days. This 50-day spin-up allows to reach equilibrium in soil P pools before the beginning of the growing season. For global simulations, the only mechanism that could make soil P pools equilibrium different from the one provided by Ringeval et al. (2024) is change in soil water content (Equation 45). For site-specific simulations, both the change in soil P pools at the beginning of the year and soil properties involved in soil P dynamics parameterization could lead to a new equilibrium.

2.5.2 | Site Description and Site-Specific Simulations

GPCROP simulation was carried out on a given site for the comparison with measurements performed in a long-term P fertilization experiment. In that case, GPCROP input relative to timing and length of the growing season, some soil properties (soil texture, pH, organic matter), initial soil P pools and main soil P inputs (mineral and manure fertilizers) were prescribed to the model to be representative to the site conditions (Table 3). One parameter of GPASOIL ($C_{P,\infty}$) was also tuned to allow the model to mimic observed soil solution P concentration measured at that site. The long-term P fertilization experiment is described in Plénet et al. (2000) and the data were provided in Morel et al. (2021). Information about the root:shoot ratio was provided by Mollier (1999). The experiment was performed in 1995–1997 at Carcarès Sainte Croix in the Southwest of France (lat. 43°52′N, long. 0°44′W, alt. 55 m). The so-called Tartas trial was initiated in 1972 and continuously cultivated in maize (*Zea mays* L.) harvested for grains under irrigated conditions. Three P fertilization treatments have been applied continuously since 1972: 0 kgP ha^{-1} yr^{-1} (treatment P0), 1.5 times the amount of P exported annually

TABLE 3 | GPCROP input.

Input	Use in GPCROP	Dataset/information used for site-scale simulations (Tartas)	Dataset/information used for global simulations
Planting day	Begin of the growing season	Value (April, 22th) was provided by Plénet et al. (2000)	A global combination of MIRCA (Portmann et al. 2010) and SAGE (Sacks et al. 2010) as provided by Elliott et al. (2015) for the GGCMs intercomparison
Day of crop maturity/harvest	End of the growing season	Value (September, 30th) was provided by Plénet et al. (2000)	A global combination of MIRCA (Portmann et al. 2010) and SAGE (Sacks et al. 2010) as provided by Elliott et al. (2015) for the GGCMs intercomparison
Daily short-wave downwelling radiation	Climate forcing variable	Conditions for the grid-cell containing the site were extracted from the datasets used for global simulations	AgMERRA weather dataset provided by Ruane et al. (2015) for the GGCMI intercomparison
Daily mean temperature	Climate forcing variable	Conditions for the grid-cell containing the site were extracted from the datasets used for global simulations	AgMERRA weather dataset provided by Ruane et al. (2015) for the GGCMI intercomparison
Cropland soil P pools at the beginning of the year	Initial conditions	$P_{i\text{-lab}}$ and $P_{i\text{-sec}}$ were scaled to match the observed P Olsen (Section 2.5.2). Other pools were derived from datasets used in global simulations.	Simulations performed in Ringeval et al. (2024) (configuration 1.1) for the year 2008.
Soil P input (through chemical fertilizer, manure, atmospheric deposition and sludges) for the year considered	Soil P input	Values (0.0, 42.8, 94.3 kgP ha^{-1} yr^{-1} for P0, P1.5, P3, respectively) was provided by Plénet et al. (2000)	See Ringeval et al. (2024).
Soil properties	Involved in parameterizations driving the exchange between soil P pools	Soil texture (6% clay, 13.5% silt, 80.5% sand), soil organic matter (1.78%) and pH in water (5.9) provided by Plénet et al. (2000) for top 0–0.25 m were used.	Global dataset provided by Soilgrids (Poggio et al. 2021) was used, as in Ringeval et al. (2024).
Current value of unmanaged soil P pools	Involved in parameterizations driving the exchange between soil P pools	Conditions for the grid-cell containing the site were extracted from the datasets used for global simulations	Global dataset of He et al. (2023) was used, as in Ringeval et al. (2024).
Potential yield at harvest	Used as target to calibrate the parameters related to plant growth without P limitation (Table 2)	Value (13.6 tDM ha^{-1}) was provided by Plénet et al. (2000) for P3.	Values was provided by Gerber et al. (2024).

from the field by grains (42.8 kgP ha^{-1} yr^{-1} on average; treatment P1.5) and 3 times the amount of P exported annually from the field by grains (94.3 kgP ha^{-1} yr^{-1} on average; treatment P3). The experimental design was a randomized complete block with each experimental treatments replicated four times. Individual plots were 6 m wide and 30 m long. Blocks and replicates were used in our study to provide standard-deviation for each treatment (P0, P1.5, and P3).

GPCROP simulation was performed on that site for the year 1996. Model input are given in Table 3. Three GPCROP simulations were performed to represent P0, P1.5, and P3: the simulations vary through the initial soil P pools and the amount of fertilizers, both used at the beginning of the simulations. Olsen-P in the 0–0.25 m top layer was measured in 1995 and amounted to 23, 49, and 66 mgP (kg of soil)$^{-1}$ in P0, P1.5, and P3, respectively (Plénet et al. 2000). We translated these values in values of P_{i-lab} used as initial conditions through the following reasoning: P_{i-lab} represented in GPCROP corresponds to resin+bicarbonate of Hedley fractionation. Such extraction is close to P extracted by the Colwell extraction ($P_{Colwell}$) as they share the same extractant during the same duration. The study of Moody et al. (2013)

provides a relationship between Olsen-P and Colwell-P for non-calcareous soils:

$$P_{Colwell} = 2.869 \times P_{Olsen} - 2.93 \quad (47)$$

with both $P_{Colwell}$ and P_{Olsen} in mgP (kg of soil)$^{-1}$. With this relationship, P-Olsen values representative to Tartas correspond to P_{i-lab} of 63, 138, and 186 mgP (kg of soil)$^{-1}$, respectively for P0, P1.5, and P3. We translated these values in gP m^{-2} by using the bulk density used in global simulations, then used them as initial soil P pools. In GPASOIL, P_{i-lab} and P_{i-sec} interact in a short time scale and modifying only the initial value of P_{i-lab} is not enough to prescribe the soil buffering capacity. Thus, we modified also the initial value of P_{i-sec} by applying it the change of P_{i-lab} between global and site-scale simulations. Initial values for other soil P pools (P_{i-sec}, P_{i-prim}, P_{o-lab}, P_{o-sta}, P_{x-occ}) were taken from input used for global simulations.

Finally, soil solution P concentration (C_P) was measured in Tartas and amounted 0.5e^{-3}, 1.6e^{-3}, and 2.9e^{-3} gP L^{-1} for P0, P1.5, and P3, respectively. C_P simulated by GPASOIL at the beginning of the growing season differed from these values and we tuned the parameter $C_{P,\infty}$ from 0.10e^{-3} gP L^{-1} in the original model (Ringeval et al. 2024) to 0.35e^{-3} gP L^{-1} to make the C_P simulated (0.6e^{-3}, 1.7e^{-3}, and 2.7e^{-3} gP L^{-1} for P0, P1.5, and P3, respectively) close to the observed values.

2.5.3 | Global Simulations

Global simulation was performed for the year 2009, that is, the last year for which empirically derived potential yield (Gerber et al. 2024), radiation, and temperature datasets were all available. As in Ringeval et al. (2021), the planting day and the day of crop maturity/harvest were prescribed by a global combination of MIRCA (Portmann et al. 2010) and SAGE (Sacks et al. 2010) as provided by Elliott et al. (2015) for the GGCMs intercomparison, and radiation and temperature were provided by Ruane et al. (2015).

Both soil P input and P losses through erosion were provided by Ringeval et al. (2024) for that year. Soil P pools at the beginning of the year were also provided by Ringeval et al. (2024) and it is worth noting that averaged-crop values (i.e., not specific to maize) were thus used.

As in Ringeval et al. (2024), the current value of unmanaged soil P pools provided by He et al. (2023) was used to approach the ratio between different soil P pools at equilibrium, needed in the relationships to compute k-parameters. For global GPCROP simulations, soil properties (soil texture, bulk density, pH, organic matter) were prescribed from Soilgrids 2.0 (Poggio et al. 2021) as in Ringeval et al. (2024). Datasets used for input are provided in Table 3.

The number of half-degree resolution grid-cells considered in GPCROP simulations is c.a. 15,000. While 25,000 grid-cells were considered for the calibration of SIM parameters, the availability of soil P values within Ringeval et al. (2024) drove the final number of grid-cells considered. Global numbers provided in Section 3 correspond to spatial global averages by using the 2009 maize area provided by Gerber et al. (2024) as weights. It is worth noting that this excludes the grid-cells with potential yield but with no 2009 reported maize area.

2.5.4 | Uncertainty on GPCROP Simulation Results

Different sources of uncertainty are considered and are related to: SIM parameters (Table 2), GPCROP parameters (Table 1), one GPASOIL parameter ($C_{P,\infty}$, Table 1) and initial soil P pools. First, we sampled a subset of all combinations of SIM parameters allowing a match with the target yield (see Section 2.4). For global simulations, this is done to reduce the number of GPCROP simulations to perform and the associated computation costs. This subset is combined with different combinations of GPCROP parameters and different values of $C_{P,\infty}$. The strategy varies according to the simulation (site-specific or global ones) following the additional constraints at site-scale and for instance, the uncertainty in initial soil P pools is only considered at the global scale. For each global GPCROP simulation, a random value of soil P pools was chosen for each grid-cell by assuming a normal distribution and by using the standard-deviation provided by Ringeval et al. (2024). Overall, c.a. 160 GPCROP simulations are performed at the site scale. We then excluded the value of several GPCROP parameters associated with the overestimation of the P limitation as compared to the one observed at site-scale (Section 3.2 and Table 1), leading to finally consider c.a. 70 simulations at site-scale. At the global scale, 60 simulations were performed after the exclusion of the same values of few GPCROP parameters as the one exlcuded in site-specific simulations (Table 1). This number of simulations was done for each GPCROP configuration ($GPCROP_{no-intera}$, $GPCROP_{non-optim}$, and $GPCROP_{optim}$). Simulations are used to provide averages and standard-deviations.

3 | Results

For the sake of simplicity, units used in Section 3 can be different from the ones used in the above equations.

3.1 | Calibration of Plant Growth Without P Limitation

The results of the Sobol analysis for SIM parameters are given in Figure S2 at global, latitudinal band and site scales. Following the Sobol analysis for $biom_{grain}$, only the following 7 parameters are then considered in the calibration: T_{min}, max_{nleaf}, GDD_{1leaf}, RUE_{tot}, f_{grain}, SLA, and GDD_{life}. While the global sensitivity of $biom_{grain}$ to SLA was found to be low, we kept SLA in the calibration, as SLA is involved in the remobilization of P (Equation 42). The calibration of SIM parameters relied then on 3^7 simulations corresponding to all combinations of parameters possible (7 parameters with 3 values allowed per parameter, Table 2). All combinations allowing to match the (Equation 46) are kept for the following GPCROP simulations. This is done for each grid-cell in the calibration at the global scale or for the unique grid-cell in the site-specific calibration.

The results of the calibration at the global scale are given in Figure S3. The calibration allows yield at harvest simulated by

GPCROP (Figure S3b) to match the spatial distribution of potential yield given by Gerber et al. (2024) (Figure S3a). The number of GPCROP parameter combinations kept after the calibration varied between <30 (mainly in Canada and Libya) and c.a. 300 (in regions around the equator). The calibration did not succeed for c.a. 900 grid-cells (i.e., 4% of the grid-cells considered with SIM): for these grid-cells, no parameter combinations allowed fitting (Equation 46). These grid-cells where GPCROP is not able to reproduce yield found in Gerber et al. (2024) are mainly located in Sudan, the north of Quebec, and in parts of China (Figure S3c).

We investigated if there is some consistency in the calibrated values among all parameter combinations kept after calibration (Figure S4) and if this consistency makes sense in regards to commonly accepted knowledge about cultivar distribution. We consider that there is a consensus in the value of a given parameter if the same value is found for more than 75% of the combinations kept after calibration. Figure S4 indicates if the calibration success requires that some parameters have a specific value. For instance, the calibration succeeds in Northern Africa only if both the maximum number of leaves per plant (max_{nleaf}) and the fraction of daily NPP allocated to the grain (f_{grain}) have their lowest values allowed (15 and 0.4, respectively). Overall, we found that there is no consensus for most places in the World (Figure S4). f_{grain} is related to harvest index (Appendix S4) and we could expect that calibrated combinations share a high f_{grain} in developed countries. Instead, the lack of consensus found in Figure S4 would suggest that the combinations kept after calibration embedded non-realistic parameters values. This could be explained by the fact that we only constrain the grain yield, allowing the calibration many degrees of freedom for finding all parameters involved.

Calibration with data from the Tartas field experiment leads to keeping c.a. 100 parameter combinations.

3.2 | Comparison to Long-Term Field Trial

C.a. 160 GPCROP simulations were performed at site-scale by combining SIM parameters allowing the simulated yield to match the observed one with the different GPCROP parameters (Table 1). Overall, the change in yield between P1.5 and P0 simulated by GPCROP is larger than the one found in observations at Tartas (23.1% with GPCROP vs. 10.7% found in observations). The change in yield between P1.5 and P0 simulated by GPCROP varies according to the values of GPCROP parameters (Figure S5). From this sensitivity analysis, we excluded $\alpha_{PUE} = 0.9$ and $conc_{swog,def} = 4.0e^{-3}$ gP gDM^{-1} from further analysis both at site scale (reducing the number of simulations to consider from c.a. 160 to c.a. 70) and at the global scale (Table 1).

Figure 2 focused on the seasonal cycle for both the observations and $GPCROP_{optim}$ when considering the above mentioned c.a. 70 simulations (see Figure S6 for the same figure with the c.a. 160 simulations). $GPCROP_{optim}$ reproduces relatively well the observed seasonal cycle of most variables related to leaves (Figure 2a) and biomass (Figure 2b) (see Table S2 for the values of Root Mean Square Errors). Both the seasonal maximum number of leaves (Figure 2a) and final biomass in shoot and shoot without grain (Figure 2b) are underestimated with GPCROP as compared to the observations. On average, the values of max_{nleaf} kept from SIM site-specific calibration is consistent to the observed seasonal maximum number of leaves but senescence simulated in the model explains the lower seasonal maximum number of leaves (not shown). The effect of senescence on biomass in GPCROP is nevertheless small (not shown). As both biomass in shoot and in shoot without grain are underestimated, the difference (corresponding to grain biomass) is consistent with the observations, as it is the target of the calibration. Overall, $GPCROP_{optim}$ captures the delay in the seasonal cycle of n_{leaf} and LAI of P0 vs. other treatments (P1.5 and P3), as compared to the delay found in the observations, but overestimated the delay for biomass (Figure 2b). $GPCROP_{optim}$ simulates no difference between P1.5 and P3.

Almost no variation of the root:shoot ratio was simulated with $GPCROP_{optim}$ while a seasonal cycle (with first an increase over the first 10 days then a decrease) was found in the observations (Figure 2c). A larger root:shoot ratio was observed for P0 than for other treatments. A sensitivity test where only the root:shoot ratio was optimized ($GPCROP_{optim,RSR}$) (vs. an optimization of root:shoot ratio and P concentration of shoot in $GPCROP_{optim}$) lead to simulate both a seasonal cycle in the root:shoot ratio and differences between the P treatments (Figure 2c).

The model underestimates the P concentration of shoot excluding grain at the beginning of the growing season and overestimates it at the end (Figure 2e). The seasonal cycle of the P concentration of shoot excluding grain is not captured by $GPCROP_{optim}$: in its current state, the model is not able to reproduce the well-known dilution curve. With its optimization procedure, $GPCROP_{optim}$ has no benefit to decrease the P concentration of shoot excluding grain in the course of the growing season while P supply is not limiting because of larger root biomass. The fact that we do not distinguish stem and leaf could also contribute to this mismatch. In GPCROP, remobilization concerns only P contained in organs that are subjected to senescence and thus, cannot contribute to reproduce a dilution curve in the model. Grain P concentration are not allowed to vary in the model. In the observations, grain P concentration does not vary in time but is slightly different among the P treatments (Figure 2e).

In the model, P contained in biomass is driven by biomass and organ P concentration. As a consequence of the uncaptured dilution curve, $GPCROP_{optim}$ underestimates P in total shoot biomass at the beginning of the growing season and overestimates it at harvest, for treatments P0 and P1.5 (Figure 2d). Differences observed between P1.5 and P3 could be related to luxury consumption of P, a process which is not represented in our model.

Figure S7 shows the effect of the P treatments on temporal averaged variables for the observations, $GPCROP_{non-optim}$ and $GPCROP_{optim}$. Overall, $GPCROP_{optim}$ has a better fit to the observations than $GPCROP_{non-optim}$. In particular, the consideration of plant adjustments allows the reproduction of low negative effect of P0 vs. other treatments as found in the observations for LAI, n_{leaf} (Figure S7a), biomass (Figure S7b), and P in biomass (Figure S7d). Interestingly, despite the model's inability to capture the dilution curve at seasonal scale as mentioned above,

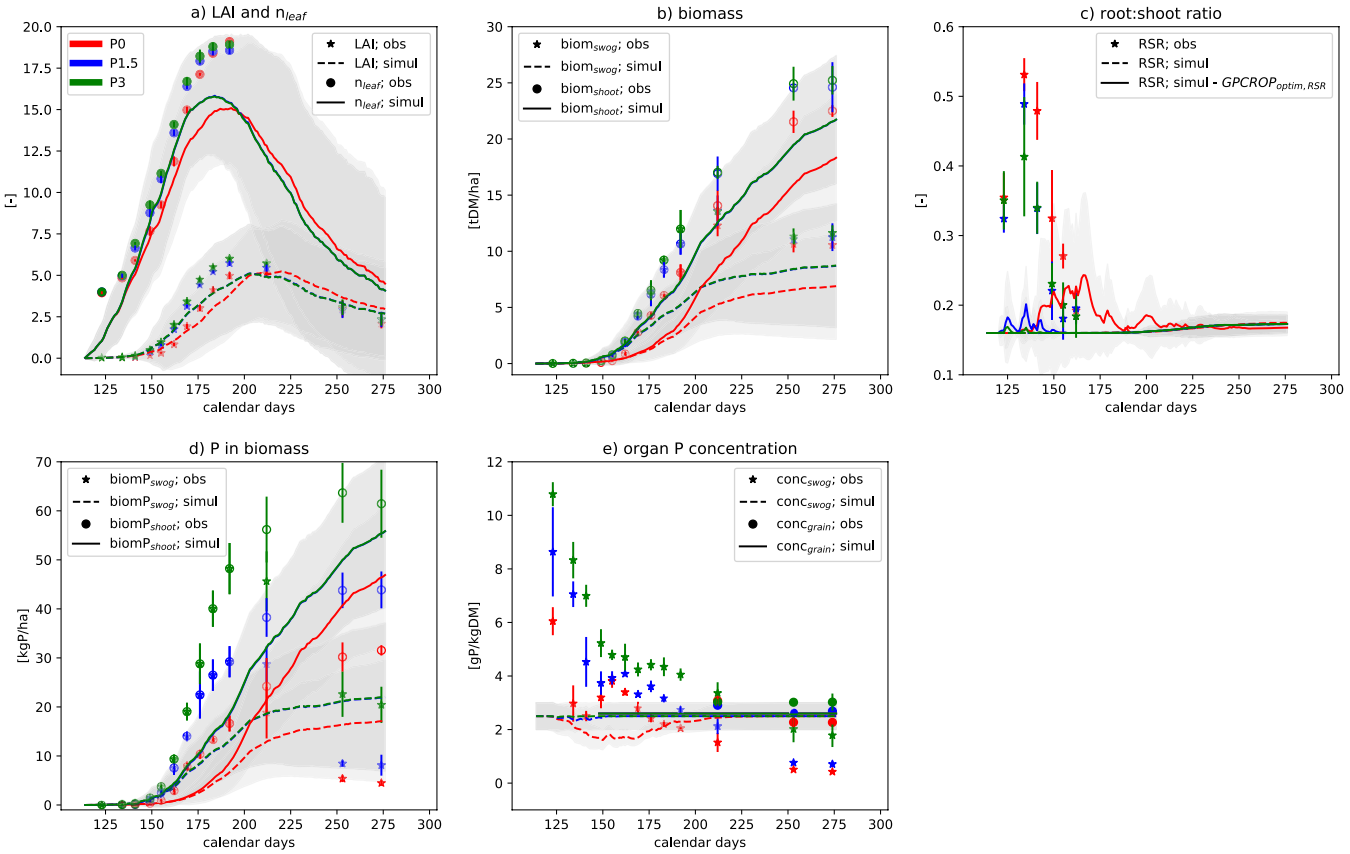

FIGURE 2 | Comparison of seasonal cycle at Tartas between observations and $GPCROP_{optim}$ for year 1996. Observations are plotted thanks to symbols while simulations are plotted with lines. Distinct colors are used for the different treatments (P0, P1.5, P3) for both observations and simulations. In panel b and c, both total shoot and shoot without grain are plotted: The difference between the both provides the information about grain. For $GPCROP_{optim}$, the grey area corresponds to two standard-deviations derived from c.a. 70 parameter combinations kept after calibration and exclusion of two parameters values at Tartas site (Section 3.2) while error-bars (equal to two standard-deviations) are used for symbols. Blue and green lines can be overlapped. In panel c, in addition to $GPCROP_{optim}$ (as in other panels), a second simulation corresponding to a sensitivity test where only the root:shoot ratio is optimized ($GPCROP_{optim,RSR}$) is plotted.

$GPCROP_{optim}$ reproduces (albeit underestimated) the lower P concentration of shoot excluding grain ($conc_{swog}$) in P0 as compared to P1.5 at the beginning of the growing season (30% in the observations vs. 20% with $GPCROP_{optim}$, Figure S7e). GPCROP shows a larger root:shoot ratio in P0 than in other treatments when averaged in time (Figure S7c) but this occurs only when the root:shoot ratio is optimized alone ($GPCROP_{optim,RSR}$) and not when its is optimized with the P concentration of shoot ($GPCROP_{optim}$).

3.3 | Model Behavior at Site Scale

The results of the three GPCROP configurations ($GPCROP_{no-intera}$, $GPCROP_{non-optim}$, and $GPCROP_{optim}$) are compared for the site-specific simulation with treatment P0 (Figure 3), without any comparison to the observations and for further understanding of the model behavior.

The first column of Figure 3 (panels a–f) shows the seasonal cycle of GPCROP variables if plant growth and P do not interact (configuration $GPCROP_{no-intera}$). The number of leaves (n_{leaf}, Figure 3a) first increases then decreases due to senescence. Organ biomass and P content of organ biomass vary accordingly (Figure 3b,c). Grain filling starts when the leaf number max_{nleaf} emerges (Figure 3a). The biomass in grain ($biom_{grain}$) reached at harvest in this configuration corresponds to yield observed at Tartas site (13.0 tDM ha^{-1} with std of 0.6 vs. 13.6 tDM ha^{-1} in the observations).

Figure 3c shows that, for the configuration without interaction between plant growth and P ($GPCROP_{no-intera}$), the P demand to sustain the plant growth (P_{demand}) is larger than the P supply by the roots (P_{supply}) at the very beginning of the growing season (between 0th and 50th days of the growing season) when roots are poorly developed, without effect on the plant growth in this configuration. However, in the configuration where plant growth and P interact $GPCROP_{non-optim}$, (2nd column of Figure 3), P limitation has a strong effect on the plant growth: plant growth is delayed until $biom_{root}$ can make P supply larger than P demand (Figure 3g,i). P limitation occurs in this configuration as soon as the number of leaves (n_{leaf}) reaches a given threshold ($n_{leaf,thresh}$). As results, yield at harvest (6.1 tDM ha^{-1}, std. of 3.7) is much smaller than in the configuration without P effect ($GPCROP_{no-intera}$) (Figure 3g). The number of leaves at harvest is, on average, larger with $GPCROP_{non-optim}$ than $GPCROP_{no-intera}$ due to the fact that P limitation postpones leaf senescence in $GPCROP_{non-optim}$. As

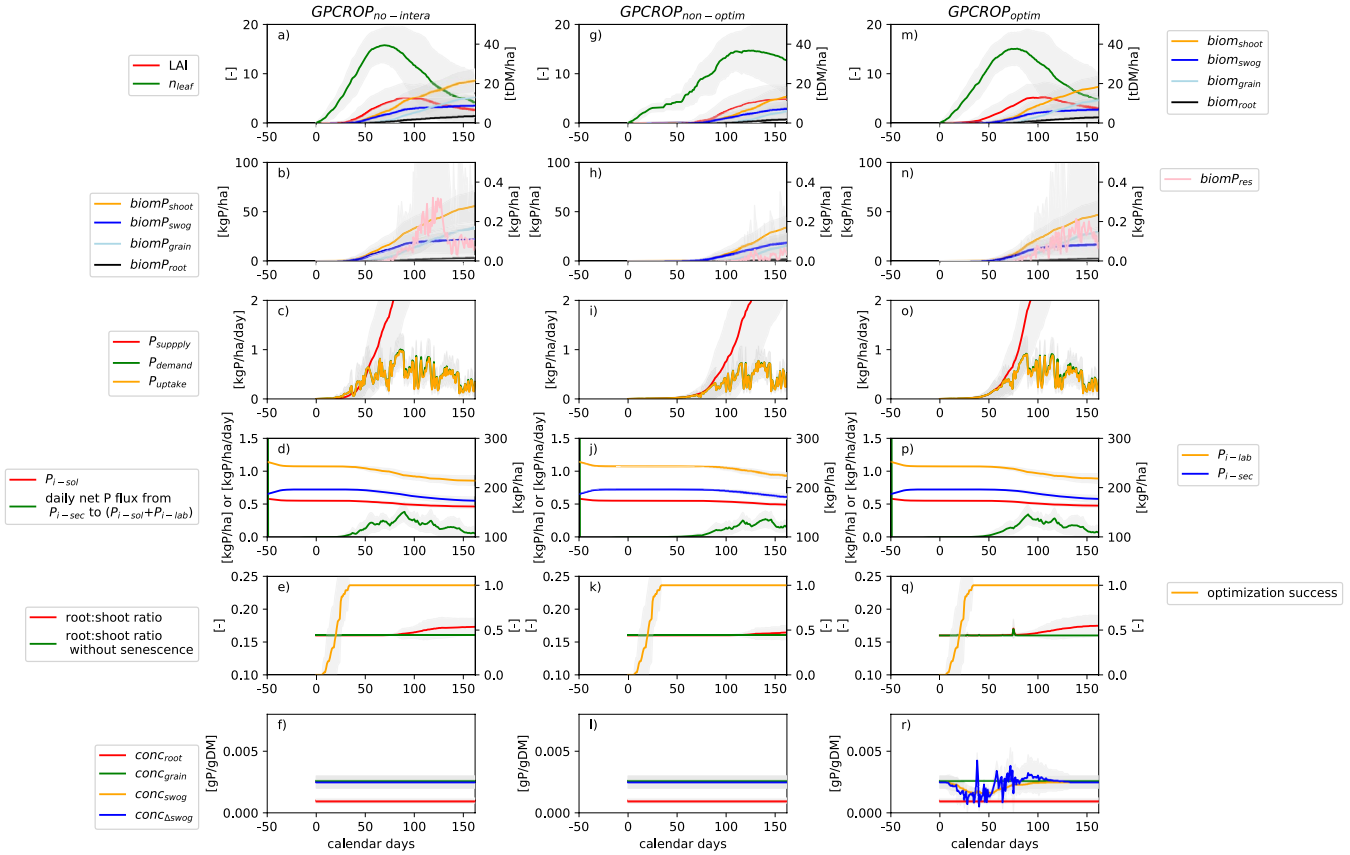

FIGURE 3 | Comparison of seasonal cycle of some variables between GPCROP$_{no-intera}$, GPCROP$_{non-optim}$, and GPCROP$_{optim}$ configurations at Tartas site for P0 treatment. Each column corresponds to a given configuration. Variables plotted are relative to biomass (line 1), P content of biomass (line 2), P supply, demand and uptake (line 3), soil P (line 4), root:shoot ratio (line 5), organ P concentration (line 6). The meaning of each variable is given in the main text except "optimization success" (line 5) which is a variable equal to 1 if the optimization procedure succeed or 0 if not (note that the optimization is used for the whole growing season once n_{leaf} is greater or equal to a given threshold called $n_{leaf,thresh}$). For some lines, panels have two *y*-axis: In that case, variables plotted with left (respectively right) y-axis are in the legend provided at left (resp. right) of the figure. For each variable, the grey area corresponds to two standard-deviations derived from c.a. 70 parameter combinations kept after calibration at Tartas site.

a sensitivity test, we checked that GPCROP$_{non-optim}$ provides similar results as an additional version of GPCROP where the different organ biomass are reduced to make the P demand consistent to the P supply without any optimization procedure, as is generally done in supply vs. demand approaches working at a daily time-step on a given site (e.g., Mollier et al. 2008). Equations corresponding to this additional version of GPCROP are given in Appendix S5.

The root:shoot ratio when considering biomass that can suffer from senescence increases slightly at the end of the growing season in all configurations (Figure 3e,k,q). Removing the effect of the senescence, the root:shoot ratio is constant in both GPCROP$_{no-intera}$ (Figure 3e) and GPCROP$_{non-optim}$ (Figure 3k). Similarly, the P concentration of shoot without grain is constant in these two versions (Figure 3f–l). In the configuration where plants can adjust to P limitations (GPCROP$_{optim}$, 3rd column of Figure 3), plants optimize allocation and P concentration of shoot without grain. The change in allocation leads to change in root:shoot ratio (Figure 3q). While the changes in both root:shoot ratio and P concentration of shoot without grain are quite small (Figure 3q,r), these changes are enough to alleviate almost totally the P limitation: plant growth is not delayed any more (Figure 3m) (contrary to GPCROP$_{non-optim}$) and the yield at harvest is very close to the one found in GPCROP$_{no-intera}$ (11.4 tDM ha^{-1}, std. of 1.8). Root:shoot ratio changes only very punctually in GPCROP$_{optim}$ and the model rather modifies the P concentration of shoot without grain. In Figure S8, we showed how the model optimizes the root:shoot ratio and the P concentration, independently or together, at the 1st day of optimization along a gradient of P limitation induced by scaling the initial soil P pools. This figure shows that, on the considered site, as soon as P concentration is allowed to vary, the optimization procedure focuses on the concentration instead of on the root:shoot ratio.

Soil P pools evolve slightly at seasonal scale (Figure 3d,j,p). Nevertheless, the model simulates a positive net flux from P_{i-sec} to P_{i-lab} (through P_{i-sol}), which buffer the decreases in P_{i-lab} due to P uptake.

3.4 | Global Simulations

A number of 60 GPCROP simulations are considered at the global scale. Optimization succeeds in more than 99% of grid cells considered in GPCROP.

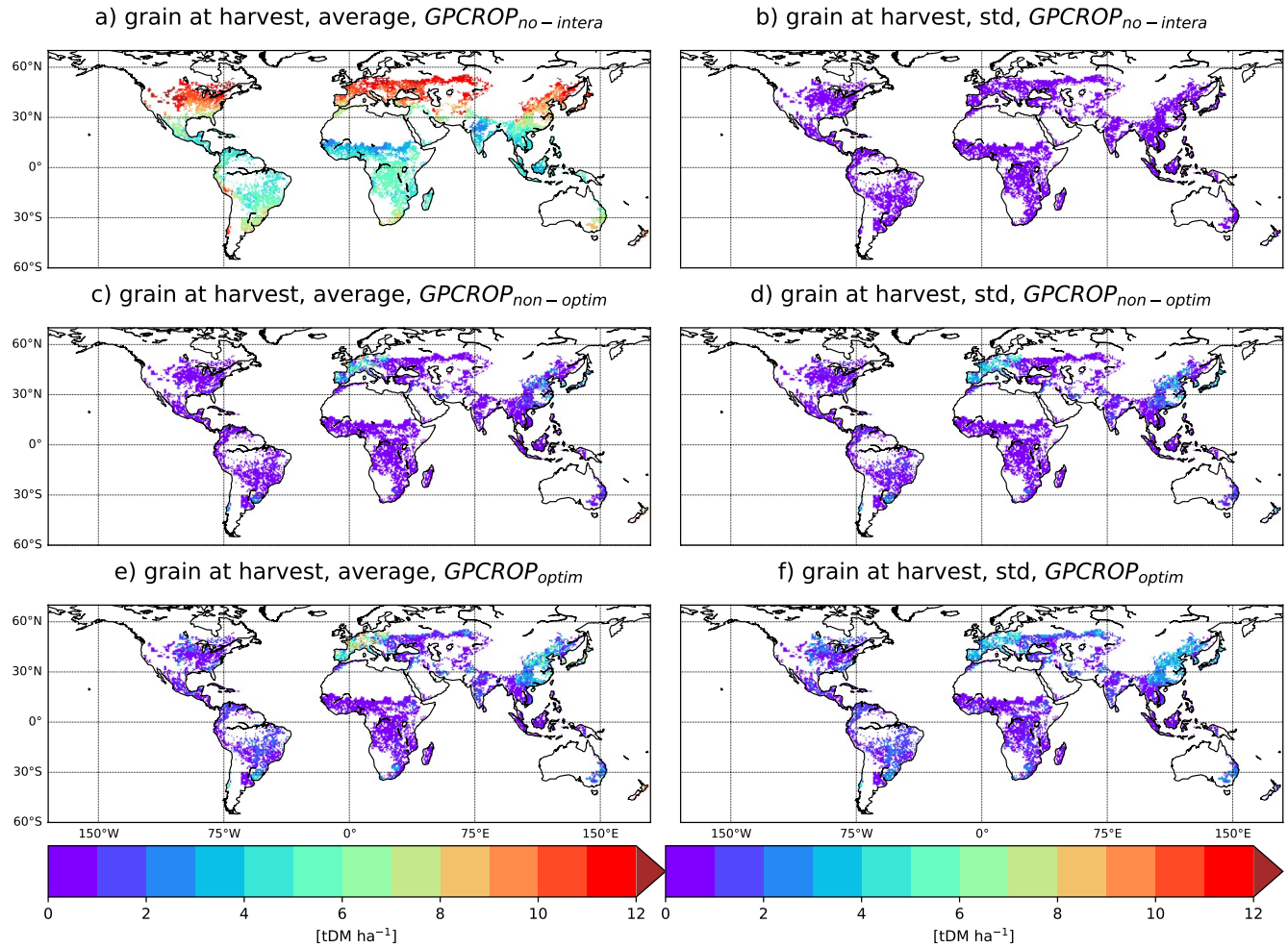

FIGURE 4 | Yield at harvest: Differences between GPCROP simulations. The grain biomass at harvest ($\text{biom}_{\text{grain}}(t = t_m)$) is given for different GPCROP configurations (potential yield: $\text{GPCROP}_{\text{no-intera}}$, yield limited by P without plant adjustements: $\text{GPCROP}_{\text{non-optim}}$, yield limited by P with plant adjustements: $\text{GPCROP}_{\text{optim}}$). Left column corresponds to average among GPCROP simulations ($n = 60$) while right columns corresponds to the standard-deviation ($n = 60$). Standard-deviation of potential yield (panel b) is almost null: All SIM parameters kept after the calibration of the plant growth without P leads to a potential yield close to one provided by Gerber et al. [2024].

When the effect of P limitation on plant growth was accounted for, the average maize yield at the global scale greatly decreased (Figure 4c, $\text{GPCROP}_{\text{non-optim}}$), as compared to the potential yield (Figure 4a, $\text{GPCROP}_{\text{no-intera}}$). The global maize production massively decreases from 877 MtDM (million of tons of dry matter) (std of 1) to 64 MtDM (std = 65) (i.e., a reduction of 92.7% with a std. of 7.4%) when combining the simulated yield with the 2009 real maize area. Taking into account plant adjustments partly alleviates the P limitation with a global production of 185 MtDM (std = 152), that is, a reduction of 78.9% (std = 17.3) as compared to the potential yield (Figure 4e). This alleviation mostly happens in Europe and China but remains spatially restricted at the global scale (Figure 4e).

We found a considerable uncertainty in GPCROP simulations as soon as P limitation is considered (Figure 4d,f). Among all parameters, the parameter $C_{P,\infty}$ (describing the equilibrium P concentration of the soil solution) is the one that contributes the most to the uncertainty (Figure 5). For instance, when splitting the 60 simulations according to the $C_{P,\infty}$ prescribed to the model, the coefficient of variation decreases from 82% ($n = 60$) to 56% ($C_{P,\infty} = 0.10e^{-3}$ gP L^{-1}, $n = 30$) and 28% ($C_{P,\infty} = 0.35e^{-3}$ gP L^{-1}, $n = 30$). In a lesser extent, the number of leaves from which interaction between plant growth and P begins ($n_{\text{leaf,thres}}$), a parameter describing the sensitivity of NPP to the P concentration (α_{PUE}) and the default P concentration of shoot without grain ($\text{conc}_{\text{swog,def}}$) contribute also to the final uncertainty (Figure 5). While we cannot precisely isolate their specific contribution, parameters involved in plant growth modeling (i.e., SIM parameters) or initial soil P seem to play a smaller role to the final uncertainty.

We also found that the beginning of the growing season, considered here as the period before grain filling starts, is key for P limitation as P roots are poorly developed at that stage. When averaged over the whole growing season, P supply is greater than the P demand in many parts of the world (brown areas in Figure S9a). But when averaged over the vegetative part of the growing season, P demand is larger than P supply almost everywhere, except in Europe (Figure S9b).

Plant adjustments involved in the partial alleviation of P limitation are shown in Figure 6. We found that the P concentration of shoot without grain is the lever mainly used by the optimization to

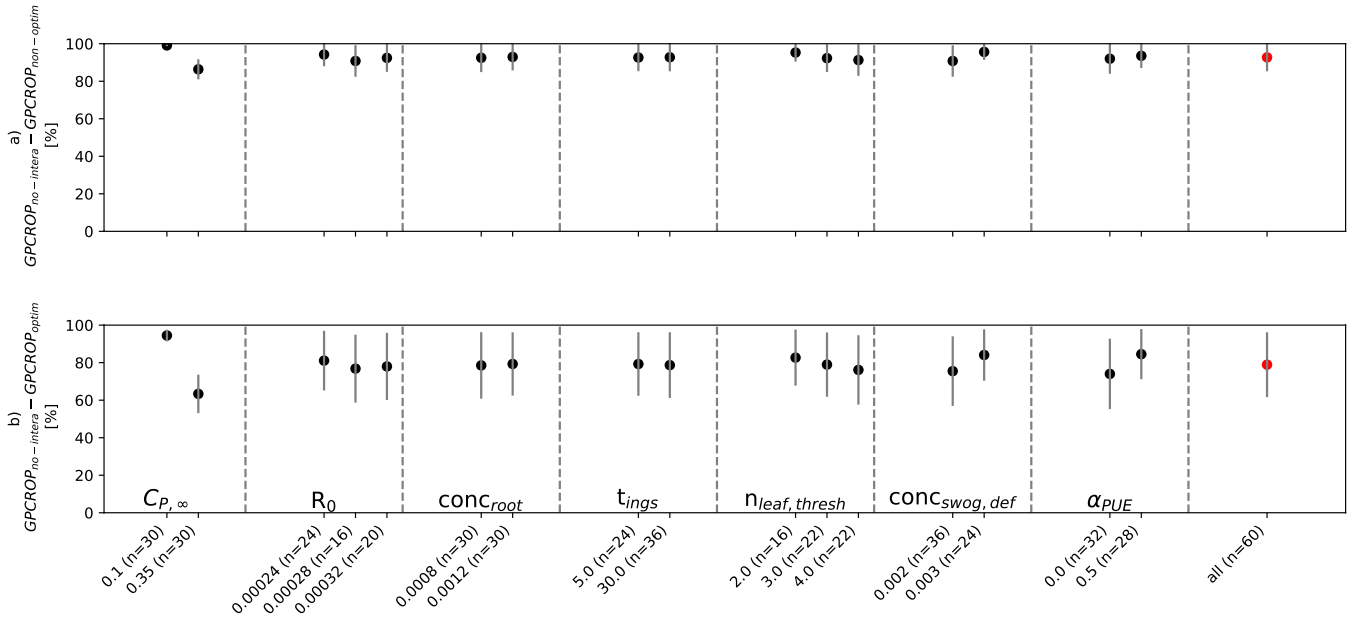

FIGURE 5 | Sensitivity of the change in global maize production to GPCROP parameter values. The change in global maize production as compared to the potential yield ($GPCROP_{no-intera}$) is given for both the configuration without ($GPCROP_{non-optim}$, top line, panel a) and with ($GPCROP_{optim}$, bottom line, panel b) plant adjustements. Changes are expressed as percent of potential production ($GPCROP_{no-intera}$). For a given panel, corresponding to a given GPCROP parameter, GPCROP simulations are splitted according to the value of the parameter considered. Average (dot symbol) and two standard-deviations (error-bar) are computed by using the subset of all GPCROP simulations sharing the same parameter value. Last panels on the right provides the change in global maize production when all simulations are considered (red dot, $n = 60$).

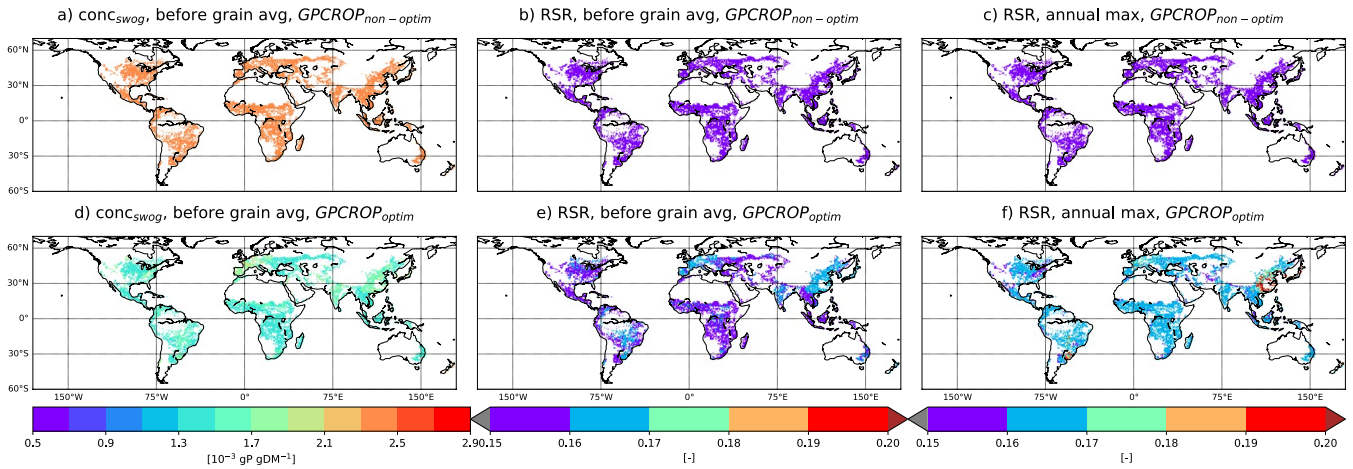

FIGURE 6 | Plant adjustments to P limitation simulated with GPCROP. Plant adjustements concern the change in P concentration of shoot without grain ($conc_{swog}$) and in the root:shoot ration (RSR). The average over the growing season before grain filling starts ("before grain avg") is given for $conc_{swog}$ (left column) and RSR (middle column). For RSR, annual maximum is given in addition (right column). Top line corresponds to root:shoot ratio and P concentration of shoot without grain in the GPCROP simulation without plant adjustements ($GPCROP_{non-optim}$): Thus, the variable are constant in space and are plotted here only to be used as standard for the value simulated by the GPCROP simulation with plant adjustements ($GPCROP_{optim}$, bottom line).

decrease the P limitation (Figure 6d vs. the default concentration in Figure 6a) instead of the change in root:shoot ratio (Figure 6e vs. the default concentration in Figure 6b). Indeed, the root:shoot ratio can be optimized, but its change is limited in time (Figure 6f).

4 | Discussion and Conclusions

For the first time, we built a model that consistently considers interactions between crop growth, plant adjustments to P limitation, and soil P dynamics in a mechanistic manner using a daily time step at the global scale. Through (i) a simple model for plant growth without P limitation and (ii) an optimization procedure for C and P allocation, the model relies on a relatively small amount of parameterization, except for soil P dynamics. We found that P limitation at the global scale reduces the global maize potential production by 78.9% (std = 17.3%), which means that the current soil P status does not allow potential yield. This is found despite the fact we considered fertilizer input for the year studied. It is likely that,

in places where other factors (nitrogen, water) are currently limiting, farmers decrease P fertilizer, leading to current soil P that cannot sustain the potential yield. It is worth noting that the aim of our work is not to provide farmer fertilizer recommendations at the local scale because of the spatial resolution and assumptions inherent in global scale modeling exercises (Haygarth and Rufino 2021). Our assumption of considering only P as a limiting factor was necessary for modeling purposes, but it prevents practical applications as this assumption can be more or less true as a function of the World regions (e.g., arid regions, regions with high share of nitrogen fixing crops). Adding P under current conditions in areas where our study found a strong P limitation does not mean that the current yield would increase. The contribution of P vs. other abiotic factors to the current yield gap at the global scale is highly uncertain (see e.g., the inability of Mueller et al. 2012 to decipher nitrogen and P) and our model could be an interesting first component of a more complete mechanistic model for global yield gap analysis.

Few studies focused on the P limitation of the current potential yield, making difficult the comparison of our results to the literature. Indeed, only few studies focused on the current production (e.g., Folberth et al. 2012; van der Velde et al. 2014; Mueller et al. 2012) while more focused on the P limitation under future scenarios (e.g., Mogollón et al. 2018, 2021; Magnone et al. 2019, 2022). Some studies focusing on current yield do not consider P alone but consider nitrogen and water in addition to P (i.e., they focus on the actual yield instead of the potential one) (Folberth et al. 2013; van der Velde et al. 2014; Mueller et al. 2012). To our knowledge, only Pradhan et al. (2015), Kvakić et al. (2018), Langhans et al. (2021) and McDowell et al. (2024) focused on the current P limitation and assumed nitrogen and water as non-limiting, and thus could be compared to the current study. All these studies have in common to find a large P limitation but the magnitudes of the P limitation found are difficult to compare because of differences in the computation of P limitation (e.g., decrease in global production due to P limitation or fertilizer needed to close the global yield gap) or in the estimates of potential yield. McDowell et al. (2024) found that an capital fertilizer application of 39 TgP (so-called "tax" in Roy et al. 2016) and additional 20 TgP yr^{-1}. for maintenance are needed to remove the P limitation in cropland. These large numbers suggest that the P limitation is widespread but cannot be easily translated into decrease in global potential crop production. Pradhan et al. (2015) found that an increase in nutrient content of crop plant between actual and potential situations would correspond to an increase of current P fertilizer application of 22%–46% but their computation does not represent at all soil P mechanisms. Langhans et al. (2021) approached the P limitation by the increase of P plant uptake induced by a quenching 20 years period (i.e., 20 years with high P fertilizer application). Global numbers of this limitation are not provided in Langhans et al. (2021) but they found that the P limitation is a global phenomena with local limitation between 40% and 80% in most places of the World (figure 1c of their study). Contrary to our study, Langhans et al. (2021) did not consider the P fertilizer application of the year considered but Kvakić et al. (2018) found that this only modified the P limitation by only 5%–10%, underlying the importance of the existing soil P supply in sustaining crop yields. Kvakić et al. (2018) found that the current yield gap due to P under current practices reach 46 (36–55)% for maize. The methods used by Kvakić et al. (2018) has many similarities to the ones used in the current study (comparison between soil P supply and plant P demand, representation of plant P uptake) but we found a larger P limitation than found by Kvakić et al. (2018). Again, potential yield can vary between the two studies (provided by one GGCM in Kvakić et al. 2018 vs. calibrated against empiral-derived potential yield in the current study) and we stress the need to better constrain the potential yield in global scale modeling. More important, our work underlines the importance in considering interactions between plant growth and soil P dynamics at daily time-step (vs. annual time-step in Kvakić et al. 2018). We found that, despite annual averages of P supply larger than P demand, taking into account the daily interactions between plant growth and soil P dynamics leads to P limitation at the beginning of the growing season, when roots are not well developed yet. This results in yield at harvest lower than potential yield. Past studies primarily relied on comparisons between annual supply versus annual demand to estimate nutrient (nitrogen, P) limitation in natural or crop ecosystems (Sun et al. 2017; Kvakić et al. 2018; Wieder et al. 2015). While this can make sense for nitrogen which is a mobile element in soil, it is likely not appropriate for P, as its uptake by the roots is limited by soil diffusion and replenishment of soil solution by more stable P pools.

We found a large limitation of potential yield by P. The yield limited by P simulated in our work is even smaller than the actual yield provided by Gerber et al. (2024) in many places of the World (Figure S10), which cannot be easily understood at first glance. Two main reasons can be invoked to explain this pattern. One is that we considered only P as the limiting factor, and taking into account other limiting factors may counterintuitively decrease the simulated P limitation on yield: if nitrogen or water is limiting at the beginning of the growing season, the slower biomass increase would spread the P demand over a longer time period than in the case without nitrogen/water limitation. This would allow time for the soil to replenish the soil solution, and this would decrease the P limitation effect on yield. How the key limiting factors interact in time and as a function of the processes involved is an open research question (Seghouani et al. 2024). The other reason is that GPCROP has some caveats that need to be addressed before we can interpret global estimates with confidence. The main caveats are non-consideration of soil iron and aluminum (hydr)oxides concentration in the soil P dynamics model, lack of representation of seed P reserves, and overly restricted plant adjustments. The soil P dynamic model at the basis of GPASOIL (Wang et al. 2022) made the parameter describing the solution P concentration at steady state ($C_{P,\infty}$) vary according to the soil iron and aluminum (hydr)oxides concentration. This was not possible when the soil P dynamic model was applied at the global scale (Ringeval et al. 2024) because of the lack of a global dataset providing the soil iron and aluminum (hydr)oxides concentration at that scale. Thus, we prescribed a spatially constant value for $C_{P,\infty}$. While the long-term (c.a. 100 year) dynamic of the soil P pools was only slightly sensitive to $C_{P,\infty}$ (Ringeval et al. 2024), we found that the annual limitation of plant growth by P at the global scale is highly sensitive to this parameter as it has an effect on the concentration of the soil P solution thus on the annual plant P uptake. This is true while the values tested in our uncertainy analysis ($0.10e^{-3}$ and $0.35e^{-3}$ gP L^{-1}) do not encompass the range of variability

provided in Wang et al. (2022) (Figure 5 of this reference). While it is difficult to know if the no-spatial representation of $C_{P,\infty}$ leads to under- or overestimation of the P limitation, the high sensitivity we found underlines the need to better represent it in the models. Earlier work started to collect soil solution P concentration values globally (Helfenstein, Jegminnat, et al. 2018; Wang et al. 2022) and this compilation could be a starting point for defining soil-specific $C_{P,\infty}$ values. Since Ringeval et al. (2024), global datasets about soil iron and aluminum (hydr)oxides concentration have started to be made available (Jia et al. 2024; Ren et al. 2024) and we stress the urgent need to further improve and expand such datasets. This was already underlined by Magnone et al. (2019, 2022) over Africa. The Wang et al. (2022) model aimed to reconcile the pools derived from the Hedley sequential chemical extraction and the mechanistic view derived from isotope exchange kinetic experiments. One step forward is to rely only on isotope exchange kinetic experiments as chemical extractions confine the representation of soil P to non-mechanistic pools. To do so, pedo-transfer functions for predicting isotope exchange kinetic parameters from soil properties are needed (Helfenstein et al. 2024) and could be implemented in GPCROP as soon as they would be available. Here again, global datasets about soil iron and aluminum (hydr)oxides concentration will be key to extrapolate globally isotope exchange kinetic parameters (Achat et al. 2016). This would allow us to simulate daily replenishment to the soil solution closer to the data derived from isotope exchange kinetic experiments (Helfenstein, Jegminnat, et al. 2018; Wang et al. 2022) while the calibration of the Wang et al. (2022) model involved such daily replenishment in combination with few other variables related to replenishment over longer time-scales and soil P pools (see Equations 27–29) of Wang et al. (2022). Our model allows interaction between plant growth and P only from a given threshold in the number of leaves ($n_{\text{leaf,tresh}}$) and our global P limitation is sensitive to this parameter. This threshold is in particular important as we found that the beginning of the growing season is a key period in the establishment of the P limitation. Considering interaction too early would overestimate the P limitation. An interesting alternative to a threshold in leaf number would be to start the simulation with some P reserve corresponding to existing P within the seed at planting day and to let the model optimize the transition between use of these reserves (autotroph period) and the uptake of P in the environment (heterotroph period) (Nadeem et al. 2014). Overly restricted plant adjustments would clearly contribute to the overestimation of P limitation. We found that GPCROP preferentially modifies the P concentration of shoot (without grain) rather than the root:shoot ratio when both plant adjustments are allowed in our optimization procedure. It is visible in both site-specific and global simulations. This is particularly visible in the site-specific simulation as GPCROP put all plasticity on the P concentration and simulated a change in the root:shoot ratio only in a configuration where the P concentration is constant. More work is necessary to make the estimate of each adjustment and their respective contribution to P limitation alleviation more robust. Data about the P concentration of the increment in biomass (instead of total biomass) would be interesting for the evaluation of GPCROP. GPCROP would also be compared to other long-term trials. More work is finally necessary to assess the sensitivity of the contribution of each adjustment to the way we model the productivity sensitivity to the P concentration or to the objective of the optimization.

GPCROP has other caveats, but it is unlikely that these caveats contribute to an overestimation of the P limitation on global production: inability in simulating a dilution curve and no explicit cultivar representation. These caveats are discussed in Appendix S6. Overall, an equilibrium has to be found between parameter parsimony and the number of mechanisms to represent. The use of organizing principles (Franklin et al. 2020) such as the optimized allocation currently used in GPCROP could help to keep the number of parameters as small as possible.

All the above limitations in mind, our model could be used to further understand the global P limitation of potential yield in a mechanistic manner. Also, it could be used to investigate how much P fertilizer is required to close the yield gap (McDowell et al. 2024) or to develop different scenarios in terms of resource P management and predict their effect on global yields. Finally, coupled with approaches dealing with water and nitrogen, GPCROP could help to quantify the contribution of each abiotic limiting factor to the current yield gap.

Author Contributions

B. Ringeval: conceptualization, methodology, software, writing – original draft, writing – review and editing. **J. Demay:** methodology, writing – original draft, writing – review and editing. **J. Helfenstein:** methodology, writing – original draft, writing – review and editing. **M. Kvakić:** methodology, writing – review and editing. **A. Mollier:** resources, writing – review and editing. **M. Seghouani:** writing – review and editing. **T. Nesme:** writing – review and editing. **J. S. Gerber:** resources, writing – review and editing. **N. D. Mueller:** resources, writing – review and editing. **S. Pellerin:** writing – review and editing.

Acknowledgments

We thank Mark Irvine, Tovo Rabemanantsoa, Philippe Debeake, Remi Lemaire-Patin, and Christelle Aluome for helpful discussions. This research was done by using Xubuntu, Singularity, and Python. This work has been realized with the support of MESO@LR-Platform at the University of Montpellier and of Mésocentre de Calcul Intensif Aquitain (MCIA) at the University of Bordeaux. This research was financially supported by INRAE (Institut national de recherche pour l'agriculture, l'alimentation et l'environnement) and its AgroEcoSystem division.

Conflicts of Interest

The authors declare no conflicts of interest.

Data Availability Statement

The code (GPCROP and scripts to analyze the output), model input, and model output that support the findings of this study are openly available in recherche.data.gouv.fr at https://doi.org/10.57745/JUFQJX. GPCROP is also available in the INRAE forge at https://forge.inrae.fr/umr-ispa/GPCROPcoupled/-/releases/v1.0_GCB_2025. GPASOIL input and output files required as input for GPCROP can be found at https://doi.org/10.57745/XZTW7Z. Other input is provided at https://doi.org/10.57745/JUFQJX.

References

Achat, D. L., N. Pousse, M. Nicolas, F. Brédoire, and L. Augusto. 2016. "Soil Properties Controlling Inorganic Phosphorus Availability: General Results From a National Forest Network and a Global Compilation of the Literature." *Biogeochemistry* 127, no. 2–3: 255–272.

Amos, B., and D. T. Walters. 2006. "Maize Root Biomass and Net Rhizodeposited Carbon." *Soil Science Society of America Journal* 70, no. 5: 1489–1503.

Barraclough, P. B., and P. B. Tinker. 1981. "The Determination of Ionic Diffusion Coefficients in Field Soils. I. Diffusion Coefficients in Sieved Soils in Relation to Water Content and Bulk Density." *Journal of Soil Science* 32, no. 2: 225–236.

Bouwman, A. F., A. H. W. Beusen, L. Lassaletta, et al. 2017. "Lessons From Temporal and Spatial Patterns in Global Use of N and P Fertilizer on Cropland." *Scientific Reports* 7: 40366.

Elliott, J., C. Müller, D. Deryng, et al. 2015. "The Global Gridded Crop Model Intercomparison: Data and Modeling Protocols for Phase 1 (v1.0)." *Geoscientific Model Development* 8, no. 2: 261–277.

Ellsworth, D. S., K. Y. Crous, M. G. De Kauwe, et al. 2022. "Convergence in Phosphorus Constraints to Photosynthesis in Forests Around the World." *Nature Communications* 13, no. 1: 5005.

Elser, J., and E. Bennett. 2011. "A Broken Biogeochemical Cycle." *Nature* 478: 29–31.

Folberth, C., T. Gaiser, K. C. Abbaspour, R. Schulin, and H. Yang. 2012. "Regionalization of a Large-Scale Crop Growth Model for Sub-Saharan Africa: Model Setup, Evaluation, and Estimation of Maize Yields." *Agriculture, Ecosystems & Environment* 151: 21–33.

Folberth, C., N. Khabarov, J. Balkovič, et al. 2020. "The Global Cropland-Sparing Potential of High-Yield Farming." *Nature Sustainability* 3, no. 4: 281–289.

Folberth, C., H. Yang, T. Gaiser, K. C. Abbaspour, and R. Schulin. 2013. "Modeling Maize Yield Responses to Improvement in Nutrient, Water and Cultivar Inputs in Sub-Saharan Africa." *Agricultural Systems* 119: 22–34.

Franklin, O., S. P. Harrison, R. Dewar, et al. 2020. "Organizing Principles for Vegetation Dynamics." *Nature Plants* 6, no. 5: 444–453.

Gerber, J. S., D. K. Ray, D. Makowski, et al. 2024. "Global Spatially Explicit Yield Gap Time Trends Reveal Regions at Risk of Future Crop Yield Stagnation." *Nature Food* 5, no. 2: 125–135.

Gerten, D., V. Heck, J. Jägermeyr, et al. 2020. "Feeding Ten Billion People Is Possible Within Four Terrestrial Planetary Boundaries." *Nature Sustainability* 3: 200–208.

Haygarth, P. M., and M. C. Rufino. 2021. "Local Solutions to Global Phosphorus Imbalances." *Nature Food* 2, no. 7: 459–460.

He, X., L. Augusto, D. S. Goll, et al. 2023. "Global Patterns and Drivers of Phosphorus Fractions in Natural Soils." *Biogeosciences* 20, no. 19: 4147–4163.

Helfenstein, J., J. Jegminnat, T. McLaren, et al. 2018. "Soil Solution Phosphorus Turnover: Derivation, Interpretation, and Insights From a Global Compilation of Isotope Exchange Kinetic Studies." *Biogeosciences* 15: 105–114.

Helfenstein, J., B. Ringeval, F. Tamburini, et al. 2024. "Understanding Soil Phosphorus Cycling for Sustainable Development: A Review." *One Earth* 7: S2590332224003737.

Helfenstein, J., F. Tamburini, C. von Sperber, et al. 2018. "Combining Spectroscopic and Isotopic Techniques Gives a Dynamic View of Phosphorus Cycling in Soil." *Nature Communications* 9, no. 1: 3226.

Jia, N., L. Li, H. Guo, and M. Xie. 2024. "Important Role of Fe Oxides in Global Soil Carbon Stabilization and Stocks." *Nature Communications* 15, no. 1: 10318.

Kvakić, M., S. Pellerin, P. Ciais, et al. 2018. "Quantifying the Limitation to World Cereal Production due to Soil Phosphorus Status." *Global Biogeochemical Cycles* 32: 143–157.

Kvakić, M., G. Tzagkarakis, S. Pellerin, et al. 2020. "Carbon and Phosphorus Allocation in Annual Plants: An Optimal Functioning Approach." *Frontiers in Plant Science* 11: 149.

Langhans, C., A. H. W. Beusen, J. M. Mogollón, and A. F. Bouwman. 2021. "Phosphorus for Sustainable Development Goal Target of Doubling Smallholder Productivity." *Nature Sustainability* 5, no. 1: 57–63.

Li, H., A. Mollier, N. Ziadi, Y. Shi, L.-E. Parent, and C. Morel. 2017. "The Long-Term Effects of Tillage Practice and Phosphorus Fertilization on the Distribution and Morphology of Corn Root." *Plant and Soil* 412, no. 1–2: 97–114.

Lun, F., J. Liu, P. Ciais, et al. 2018. "Global and Regional Phosphorus Budgets in Agricultural Systems and Their Implications for Phosphorus-Use Efficiency." *Earth System Science Data* 10, no. 1: 1–18.

MacDonald, G. K., E. M. Bennett, P. A. Potter, and N. Ramankutty. 2011. "Agronomic Phosphorus Imbalances Across the World's Croplands." *Proceedings of the National Academy of Sciences* 108, no. 7: 3086–3091.

Magnone, D., V. J. Niasar, A. F. Bouwman, A. H. W. Beusen, S. E. A. T. M. Van Der Zee, and S. Z. Sattari. 2019. "Soil Chemistry Aspects of Predicting Future Phosphorus Requirements in Sub-Saharan Africa." *Journal of Advances in Modeling Earth Systems* 11, no. 1: 327–337.

Magnone, D., V. J. Niasar, A. F. Bouwman, A. H. W. Beusen, S. E. A. T. M. Van Der Zee, and S. Z. Sattari. 2022. "The Impact of Phosphorus on Projected Sub-Saharan Africa Food Security Futures." *Nature Communications* 13, no. 1: 6471.

Margenot, A. J., S. Zhou, S. Xu, et al. 2024. "Missing Phosphorus Legacy of the Anthropocene: Quantifying Residual Phosphorus in the Biosphere." *Global Change Biology* 30, no. 6: e17376.

Martre, P., S. Dueri, J. R. Guarin, et al. 2024. "Global Needs for Nitrogen Fertilizer to Improve Wheat Yield Under Climate Change." *Nature Plants* 10, no. 7: 1081–1090.

McDowell, R. W., P. Pletnyakov, and P. M. Haygarth. 2024. "Phosphorus Applications Adjusted to Optimal Crop Yields Can Help Sustain Global Phosphorus Reserves." *Nature Food* 5, no. 4: 332–339.

Mogollón, J., A. Beusen, H. Van Grinsven, H. Westhoek, and A. Bouwman. 2018. "Future Agricultural Phosphorus Demand According to the Shared Socioeconomic Pathways." *Global Environmental Change* 50: 149–163.

Mogollón, J. M., A. F. Bouwman, A. H. W. Beusen, L. Lassaletta, H. J. M. Van Grinsven, and H. Westhoek. 2021. "More Efficient Phosphorus Use Can Avoid Cropland Expansion." *Nature Food* 2, no. 7: 509–518.

Mollier, A. 1999. "Croissance Racinaire du Mais (*Zea mays* L.) Sous Deficience en Phosphore. Etude Experimentale et Modelisation. PhD Thesis. Thèse de Doctorat Dirigée par Pellerin, Sylvain Sciences Biologiques et Fondamentales Appliquées. Psychologie Paris 11."

Mollier, A., P. De Willigen, M. Heinen, C. Morel, A. Schneider, and S. Pellerin. 2008. "A Two-Dimensional Simulation Model of Phosphorus Uptake Including Crop Growth and P-Response." *Ecological Modelling* 210, no. 4: 453–464.

Moody, P. W., S. D. Speirs, B. J. Scott, and S. D. Mason. 2013. "Soil Phosphorus Tests I: What Soil Phosphorus Pools and Processes Do They Measure?" *Crop and Pasture Science* 64, no. 5: 461.

Morel, C., D. Plénet, and A. Mollier. 2021. "Calibration of Maize Phosphorus Status by Plant-Available Soil P Assessed by Common and Process-Based Approaches. Is It Soil-Specific or Not?" *European Journal of Agronomy* 122: 126174.

Mueller, N. D., J. S. Gerber, M. Johnston, D. K. Ray, N. Ramankutty, and J. A. Foley. 2012. "Closing Yield Gaps Through Nutrient and Water Management." *Nature* 490, no. 7419: 254–257.

Müller, C., J. Elliott, D. Kelly, et al. 2019. "The Global Gridded Crop Model Intercomparison Phase 1 Simulation Dataset." *Scientific Data* 6, no. 1: 50.

Nadeem, M., A. Mollier, C. Morel, L. Prud'homme, A. Vives, and S. Pellerin. 2014. "Remobilization of Seed Phosphorus Reserves and

Their Role in Attaining Phosphorus Autotrophy in Maize (*Zea mays* L.) Seedlings." *Seed Science Research* 24, no. 3: 187–194.

Obersteiner, M., J. Peñuelas, P. Ciais, M. van der Velde, and I. A. Janssens. 2013. "The Phosphorus Trilemma." *Nature Geoscience* 6, no. 11: 897–898.

Plénet, D., S. Etchebest, A. Mollier, and S. Pellerin. 2000. "Growth Analysis of Maize Field Crops Under Phosphorus Deficiency." *Plant and Soil* 223, no. 1–2: 119–132.

Poggio, L., L. M. de Sousa, N. H. Batjes, et al. 2021. "SoilGrids 2.0: Producing Soil Information for the Globe With Quantified Spatial Uncertainty." *Soil* 7, no. 1: 217–240.

Portmann, F. T., S. Siebert, and P. Döll. 2010. "MIRCA2000-Global Monthly Irrigated and Rainfed Crop Areas Around the Year 2000: A New High-Resolution Data Set for Agricultural and Hydrological Modeling: MONTHLY IRRIGATED AND RAINFED CROP AREAS." *Global Biogeochemical Cycles* 24, no. 1: GB1011.

Pradhan, P., G. Fischer, H. van Velthuizen, D. E. Reusser, and J. P. Kropp. 2015. "Closing Yield Gaps: How Sustainable Can We be?" *PLoS One* 10, no. 6: e0129487.

Ren, S., C. Wang, and Z. Zhou. 2024. "Global Distributions of Reactive Iron and Aluminum Influence the Spatial Variation of Soil Organic Carbon." *Global Change Biology* 30, no. 11: e17576.

Ringeval, B., L. Augusto, H. Monod, et al. 2017. "Phosphorus in Agricultural Soils: Drivers of Its Distribution at the Global Scale." *Global Change Biology* 23, no. 8: 3418–3432.

Ringeval, B., J. Demay, D. S. Goll, et al. 2024. "A Global Dataset on Phosphorus in Agricultural Soils." *Scientific Data* 11, no. 1: 17.

Ringeval, B., C. Müller, T. A. M. Pugh, et al. 2021. "Potential Yield Simulated by Global Gridded Crop Models: Using a Process-Based Emulator to Explain Their Differences." *Geoscientific Model Development* 14, no. 3: 1639–1656.

Rosenzweig, C., J. Elliott, D. Deryng, et al. 2014. "Assessing Agricultural Risks of Climate Change in the 21st Century in a Global Gridded Crop Model Intercomparison." *Proceedings of the National Academy of Sciences* 111, no. 9: 3268–3273.

Roy, E. D., P. D. Richards, L. A. Martinelli, et al. 2016. "The Phosphorus Cost of Agricultural Intensification in the Tropics." *Nature Plants* 2, no. 5: 16043.

Ruane, A. C., R. Goldberg, and J. Chryssanthacopoulos. 2015. "Climate Forcing Datasets for Agricultural Modeling: Merged Products for Gap-Filling and Historical Climate Series Estimation." *Agricultural and Forest Meteorology* 200: 233–248.

Sacks, W. J., D. Deryng, J. A. Foley, and N. Ramankutty. 2010. "Crop Planting Dates: An Analysis of Global Patterns." *Global Ecology and Biogeography* 19, no. 5: 607–620. https://doi.org/10.1111/j.1466-8238.2010.00551.x.

Sattari, S. Z., A. F. Bouwman, K. E. Giller, and M. K. van Ittersum. 2012. "Residual Soil Phosphorus as the Missing Piece in the Global Phosphorus Crisis Puzzle." *Proceedings of the National Academy of Sciences of the United States of America* 109, no. 16: 6348–6353.

Seghouani, M., M. N. Bravin, and A. Mollier. 2024. "Crop Response to Nitrogen-Phosphorus Colimitation: Theory, Experimental Evidences, Mechanisms, and Models. A Review." *Agronomy for Sustainable Development* 44, no. 1: 3.

Shiferaw, B., B. M. Prasanna, J. Hellin, and M. Bänziger. 2011. "Crops That Feed the World 6. Past Successes and Future Challenges to the Role Played by Maize in Global Food Security." *Food Security* 3, no. 3: 307–327.

Sun, Y., D. S. Goll, J. Chang, et al. 2021. "Global Evaluation of the Nutrient-Enabled Version of the Land Surface Model ORCHIDEE-CNP v1.2 (r5986)." *Geoscientific Model Development* 14, no. 4: 1987–2010.

Sun, Y., Y. Han, Z. Xu, J. Zhang, J. Shen, and L. Cheng. 2023. "Phosphorus Partitioning Contribute to Phosphorus Use Efficiency During Grain Filling in *Zea Mays*." *Frontiers in Plant Science* 14: 1223532.

Sun, Y., S. Peng, D. S. Goll, et al. 2017. "Diagnosing Phosphorus Limitations in Natural Terrestrial Ecosystems in Carbon Cycle Models." *Earth's Future* 5, no. 7: 730–749.

van der Velde, M., C. Folberth, J. Balkovič, et al. 2014. "African Crop Yield Reductions due to Increasingly Unbalanced Nitrogen and Phosphorus Consumption." *Global Change Biology* 20, no. 4: 1278–1288.

Walker, T. W., and J. K. Syers. 1976. "The Fate of Phosphorus During Pedogenesis." *Geoderma* 15, no. 1: 1–19.

Wang, Y., Y. Huang, L. Augusto, D. S. Goll, J. Helfenstein, and E. Hou. 2022. "Toward a Global Model for Soil Inorganic Phosphorus Dynamics: Dependence of Exchange Kinetics and Soil Bioavailability on Soil Physicochemical Properties." *Global Biogeochemical Cycles* 36, no. 3: e2021GB007061.

Wieder, W. R., C. C. Cleveland, W. K. Smith, and K. Todd-Brown. 2015. "Future Productivity and Carbon Storage Limited by Terrestrial Nutrient Availability." *Nature Geoscience* 8, no. 6: 441–444.

Willigen, P. D., and M. v. Noordwijk. 1994. "Mass Flow and Diffusion of Nutrients to a Root With Constant or Zero-Sink Uptake I. Constant Uptake II. Zero-Sink Uptake." *Soil Science* 157: 171–175.

Zaehle, S., and D. Dalmonech. 2011. "Carbon–Nitrogen Interactions on Land at Global Scales: Current Understanding in Modelling Climate Biosphere Feedbacks." *Current Opinion in Environmental Sustainability* 3, no. 5: 311–320.

Zhang, J., A. H. W. Beusen, D. F. Van Apeldoorn, J. M. Mogollón, C. Yu, and A. F. Bouwman. 2017. "Spatiotemporal Dynamics of Soil Phosphorus and Crop Uptake in Global Cropland During the 20th Century." *Biogeosciences* 14, no. 8: 2055–2068.

Supporting Information

Additional supporting information can be found online in the Supporting Information section. **Data S1:** gcb70485-sup-0001-DataS1.pdf.